RADIOLUMINESCENCE OF RARE GASES

(review article)

M. Salete S. C. P. Leite
Departamento de Física, Universidade de Coimbra
3000 Coimbra, Portugal

(Received 8 April 1980)

CONTENTS

1 — INTRODUCTION

The passage of an ionizing radiation through a material medium gives rise to the ionization and excitation of its atoms or molecules. The electronic energy of excitation is then dissipated non radiatively through collisional processes or internal extinction, or is radiatively emitted as photons. This luminescence excited by an intense flux of ionizing radiation, or radioluminescence, is a well known phenomenon since the early days of radioactivity. However it was not until the fifties that the radioluminescence of gases, particularly that of rare gases, started being used on a new particle detector – the scintillation counter – a system essentially formed by the association of a cell containing the gaseous scintillator and a photomultiplier. Its development was extremely fast due to the considerable progresses achieved in the construction of new photomultiplier tubes: higher gain, spectral sensitivity of the photocathode enlarged towards UV and IR, lower noise, etc. [1].

In the last few years, much work was devoted to the development of these detectors and to the improvement of its performance, leading to detectors with excellent characteristics from the point of view of linearity, time and energy resolution and count rate capabilities. However, most of the published works in this area have an essentially technological nature and it was not until recently that some more detailed spectroscopic studies have been performed trying to elucidate the fundamental mechanisms involved in the radioluminescence of rare gases.

A clear understanding of the processes occuring when the ionizing radiation interacts with the matter is essential for the development of the scintillation gas counters or for any other devices making use of the same effect. The knowledge of the spectral distribution of the emitted luminescence, of its mechanism, the influence of pressure and of electric and magnetic fields is fundamental to optimize the response from those systems. In the last few years, due to the large increase in the range of applications of radioluminescence of rare gases, such as, among others, the use of the scintillation gas counters as particle detectors in several fields of physics, the development of new gaseous lasers [2], particularly nuclear pumped rare gas lasers, the detection of ultratraces of atmospheric materials and harmful heavy metals through radioluminescence [3], the study of the mechanism and kinetics of the processes involved became an urgent task to be performed [4].

Considerable progresses were obtained in the last few years in this field, and although the mechanism and kinetics are not yet fully established [5] - [8] one thinks that the physics of the processes involved is now understood, at least qualitatively.

The main purpose of the present work is to briefly review the elementary processes occurring when rare gases are submitted to an ionizing radiation, and to consider the evolution of the atomic states directely excited, that is, the path of the excitation energy. From a review of the literature, a probable mechanism for the radioluminescence of rare gases is established. This review covers the most relevant works published in this field, though in no way trying to be exhaustive.

2 — INTERACTION OF IONIZING PARTICLES WITH MATTER, WITH PARTICULAR REFERENCE TO RARE GASES

Light emission in a medium submitted to the action of a charged particle is the last stage of a complex set of elementary phenomena, that can be analised considering three main steps:

— in the first one, very brief ($\sim 10^{-9}$ s in a gas at atmospheric pressure), the primary particle and the secondary electrons released from the material by ionization are slowed down and they create primary states of activation having a large energy

— in the second stage, the directly excited and ionized states either go into the emitting states (radiative states) or deexcite through other channels

— finally the decay of the radiative states.

When a particle moves through a gaseous medium its energy is lost essentially by elastic and inelastic collisions with the atoms and/or molecules of the medium and by radiative losses (bremstrahlung). Elastic collisions are efficient only for heavy particles at the end of their paths (cross section varies with V_0^{-2}, V_0 being the particle velocity), while bremstrahlung emission is significant only when the kinetic energy of the particle is very much larger than its energy at rest. The interaction of charged particles with matter takes place mainly with atomic electrons, so that the primary products are atoms or molecules excited or ionized and electrons liberated in the ionization process [9] [10]. These electrons, on the other hand, can also ionize and excite the medium until they become sub-ionization or sub-excitation electrons, respectively. The energy of the sub-excitation electrons is finally lost in elastic collisions (or even in inelastic collisions others than those involving electronic excitations, such as vibrational and rotational excitations in molecules) until they are thermalized and eventually recombine in the medium or at the cell walls. It is a well known fact that the kinetic energy of the electrons liberated in the ionization processes directly induced by the primary particle constitutes the largest part of the energy dissipated in the medium. Usually there is no distinction between the effects of the incident particle and those of the secondary electrons, and a considerable amount of the final effects (specially electronic excitations) are due to the secondary electrons [11].

The knowledge of the excitation and ionization cross sections as a function of the nature and kinetic energy of the incident particles would allow the determination of the species formed and their relative proportions [12]. Unfortunately, this detailed and explicit information is scanty [12]-[18]. Calculated values come usually from the Born-Bethe approximation [15]; according to this approximation, cross sections tor the electronic transitions under swift particles collision are proportional to f/E, f being the optical oscillator strength for the transition under consideration and E its energy. This cross section varies with the velocity of the incident particle as $V_0^{-2} \log V_0$. In the rare gases, most of the oscillator strength lies in the ionization continuum, so ionized atoms are expected to largely exceed excited atoms. For Ar, for example, the Kuhn-Thomas rule gives a theoretical total oscillator strength of 18, and according to Samson and Kelly [19] 83% lies in the ionization continuum.

The knowledge of the oscillator strengths for several energy levels would allow the population of these states to be determined. Oscillator strengths are not at all easy to calculate theoretically, and the values presently known for some levels of a few rare gases (for others there are no calculated values at all) are currently being improved by the introduction of new techniques of calculation and more correct approximations for the wave functions of the states concerned.

The role of the secondary electrons in the production of primary states of activation is essential, particularly in the creation of excited states. The energy spectra of these electrons (degradation spectra) is generally not well known though Platzman's calculations for He [17], [20] - [24] emphasize the large range of energies involved; so the calculation of the primary states of activation is a very complicated task [25] [26] inasmuch as electrons can also induce (through electron exchange) optically forbidden transitions, although these are significant only for slow electrons. Detailed calculations involving an energy bookkeeping from the incident particles and the secondary electrons would be of extreme utility, but to our knowledge it has been tried only for He [17] [20] [24]. In fig. 1 and table I [27] are

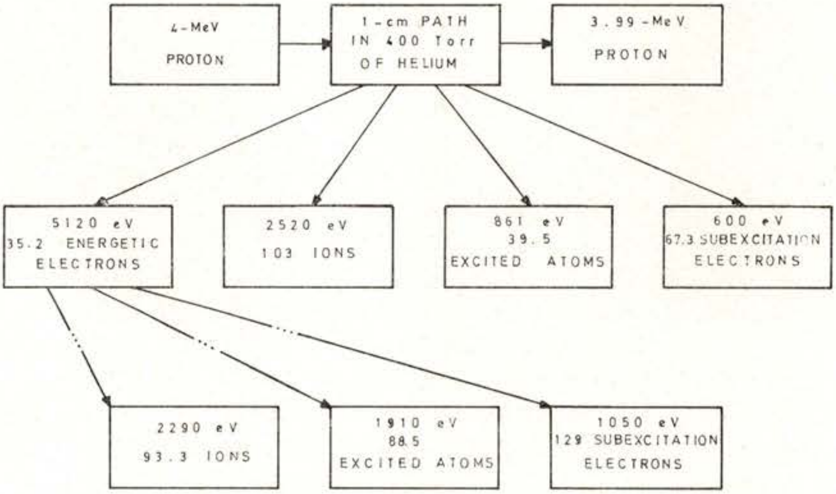

Fig. 1 — Calculated energy degradation when a 4-MeV proton loses a fraction of its energy in helium. The energies given are the portions of the 9101 eV lost by the proton that appear in the species indicated. The numbers of those species produced are also indicated (taken from ref. [27]).

represented, as an illustration, the number of ions and excited states obtained when a 4 MeV proton traverses 1 cm in He at 400 torr. The dominant role of secondary electrons is well underlined.

TABLE I — Average populations resulting when a 1 MeV-proton has a 1-cm path in 400 torr of helium (from ref. [27]).

Products	Primary proton	Secondary electrons
$2\ ^1S$	1.40	8.82
$3\ ^1S$	0.31	1.71
$2\ ^1P$	25.30	27.60
$3\ ^1P$	6.24	6.32
$3\ ^1D$	0.07	1.03
$2\ ^3S$	—	16.00
$2\ ^3P$	—	1.56
$3\ ^3P$	—	8.67
$3\ ^3D$	—	1.77
Other atomic levels	6.08	1.85
Total	39.40	88.53
Ions	103	93.3

Experimental values of cross sections for ionization and excitation come, in general, from measurements of energy losses by electron impact [12]. The strong and detailed correlation of the results at high energies with the optical absorption coefficients for a given gas confirmates that the observed peaks of the high energy spectra correspond to optically allowed transitions; at low energies, some additional peaks appear due to forbidden transitions [12] [28]. For argon, for example, excited under 50 KeV electrons impact, the levels preferentially reached are those represented in table II [28] [29]. Agreement between relative values of peak intensities and f/E relative values is quite good [16] if uncertainties in oscillator strengths are kept in mind.

In fig. 2 [30] observed cross-sections for excitation of the $3\ ^1P$ state of helium by electron impact are compared with the ones calculated from the Born-Bethe approximation: agreement is good for high energies (usually for energies $>$ 200 eV) but poor for low ener-

TABLE II — Comparison of oscillator strengths for some discrete levels of argon with relative intensities of loss peaks under electron impact

Loss Peaks Energy E (eV) ref. [12]	Atomic States ref. [12]	Relative Intensity of Loss Peaks ref. [29]	Experimental Oscillator Strength (f_{exp}) ref. [16]	Theoretical Oscillator Strength (f_{theor}) ref. [16]	f_{exp}/E	f_{theor}/E	$(f_{exp}/E)_{rel}$	$(f_{theor}/E)_{rel}$
11.62	4s $^3P_1$	0.31	0.0633 (0.059–0.067)	0.059 (0.049–0.080)	0.0055	0.0051	0.26	0.20
11.83	4s $^1P_1$	1.00	0.250 (0.228–0.280)	0.300 (0.200–0.300)	0.021	0.025	1.00	1.00
14.10	5s $^3P_1$, 3d $^3D_1$	0.27	0.130	0.112	0.0092	0.0079	0.43	0.32
14.26	5s $^1P_1$	0.23	0.130	0.112	0.0091	0.0079	0.43	0.31
14.86	6s $^3P_1$, 4d $^3D_1$	0.11	0.06	0.053	0.0040	0.0036	0.19	0.14

Note: Values of f_{exp} and f_{theor} in brackets stress the uncertainties in oscillator strengths gies. We must stress, however, the fact that for low energies cross sections are poorly known and there are no satisfactory theories [30].

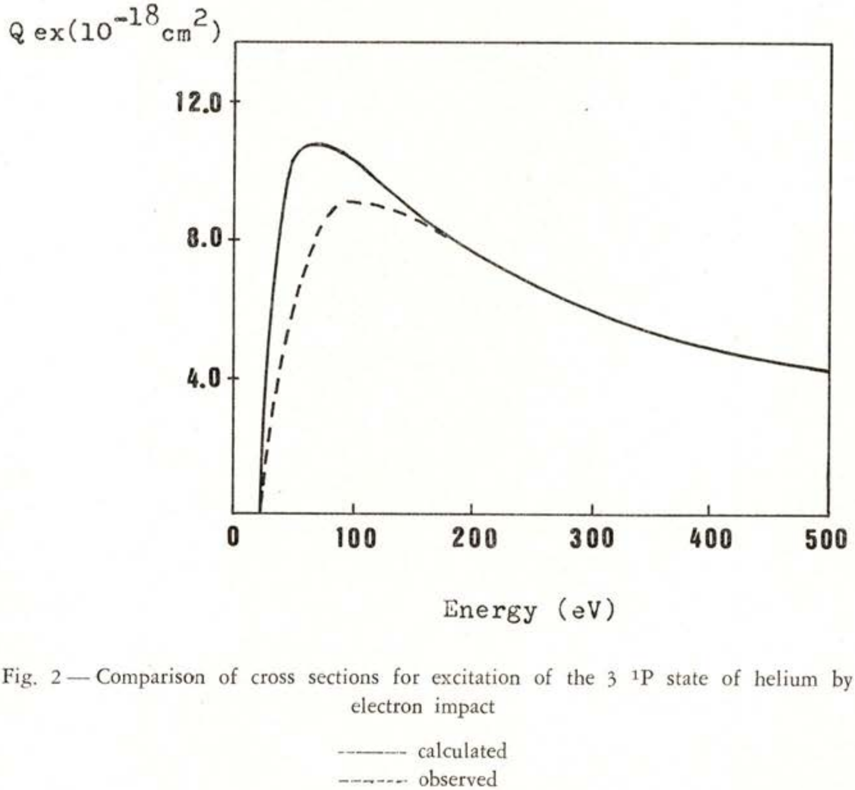

Fig. 2 — Comparison of cross sections for excitation of the 3 ^{1}P state of helium by electron impact

——— calculated

– – – – observed

(taken from ref. [30]).

In fig. 3 [31] curves for the variation of ionization cross section for single, double and total ionization as a function of the energy of the incident electrons are represented for the lighter rare gases. For He and Ne, the usual approximation of neglecting the formation of multiple charge ions is justifiable, but not so much for Ar: recent measurements under 2 KeV electron impact [32] indicate a relation $Ar^{++}/Ar^{+} = 5\%$. The effect is still more pronounced for Kr and Xe [32]. In fig. 4 are indicated cross sections of excitation and ionization of He by α particles [33]. It is clear that the amount of energy spent in the formation of ions is larger than the one used for the excitation of several levels, and that the level preferentially excited is the state 2 ^{1}P, bound to the ground state by the largest oscillator strength.

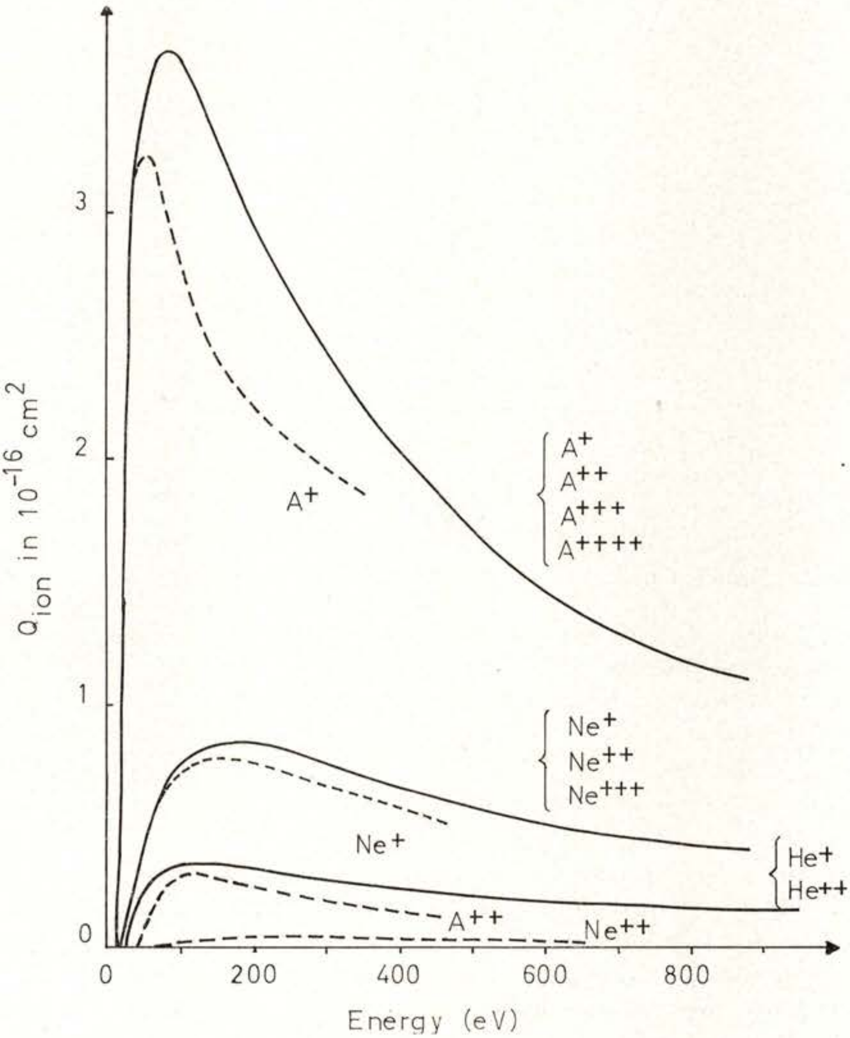

Fig. 3 — Cross sections for single and multiple ionization of helium, neon and argos by electron impact (taken from ref. [31]).

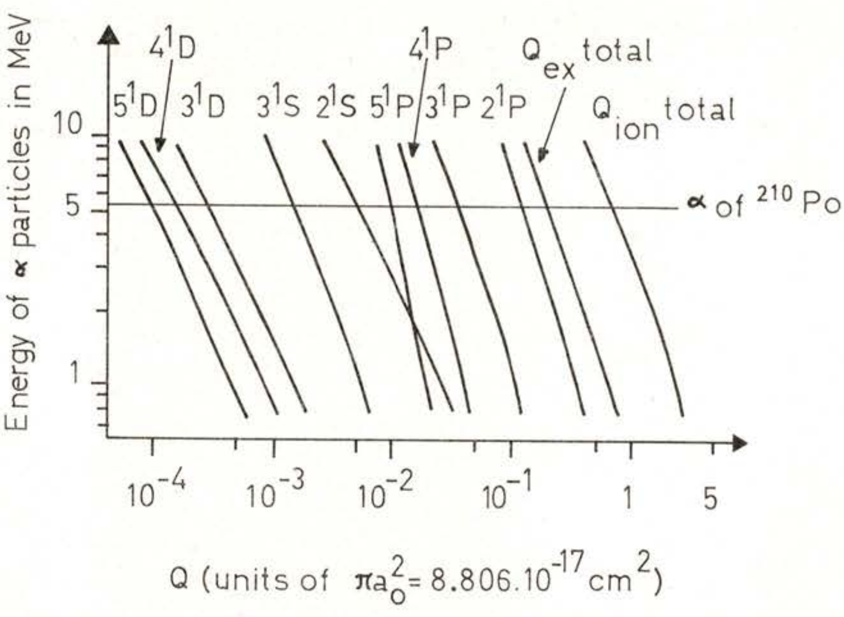

Fig. 4 — Cross sections for excitation and ionization of helium by α-particles (Born approximation) (taken from ref. [33]).

3 — EVOLUTION OF THE PRIMARY STATES

3.1 — *Spectra observed*

After the first stage, during which the primary activated states are created, the medium contains:

- ions, excited or not, mostly singly charged
- excited atoms in several levels
- electrons
- neutral atoms.

In the absence of atomic collisions (gas at very low pressure) excited atoms would deexcite radiatively with a probability inversely proportional to the lifetime of the excited state; but in a gas under pressure, collisions due to thermal agitation become very important. The primary activated atoms participate then in binary and ternary reactions, that compete with the emission of atomic lines, reducing the natural lifetime of the excited states; other species may then be created whose radiative deactivation contributes to the observed radioluminescence [10], [33] - [35].

For the rare gases excited by swift charged particles, most of the irradiated energy lies in the VUV [36]. The specific luminescence $d\varepsilon/dx$, defined as the energy radiated per unit distance along the particle track, is taken very often as a measure of the luminescent yield, as well as the luminescence yield $d\varepsilon/dE$, defined as the energy radiated per unit of energy lost in the medium by the ionizing particle. According to Hurst [36], $d\varepsilon/dx$ for the noble gases is an appreciable fraction of the total stopping power dE/dx. For argon at 400 torr, for instance, under excitation by impact with 4 MeV protons, 29 % of the energy lost by the protons appears as emission in the VUV, though this value tends to be lower for the other rare gases.

Recent measurements [37] under 5.5 MeV α-particles impact tend to corroborate this high efficiency for argon. However, if we keep in mind that the number of excited atoms formed on passage of a charged particle through argon is 40 % of the number of ions created [20], and taking 26.2 eV as the energy required to form an ion-pair in argon [36], a scintillation efficiency of 29 % would require ion-electron recombination as an additional source of excited atoms [36] [37]. Dissociative recombination (see section 3.3.3) can indeed be important and increase significantly the intensity luminescence at high pressures, particularly for the heavier rare gases [38] [39]. At pressures lower than 1 atm, however, particularly for the lighter rare gases, the effect does not seem to be so important [34] [35] [40] though experimental evidence of recombination does exist [41]. Experimental work in this field is scanty. Preliminary work in this Department tends to show that recombination at pressures lower than 1 atm is observable for Kr and Xe but unimportant for Ar, but further work on this subject is to be carried on.

The emission spectrum of a gas observed on the sequence of excitation is characteristic of the gas used, of its pressure and of the excitation process. The emission spectrum of the rare gases (except He) in the VUV presents two reasonably sharp lines in the wavelength region of their first excited states that are resonance radiation and two continua emissions at longer wavelengths, known as the first and the second continuum. The relative amount of those spectral components depends on the pressure as well as on the excitation conditions.

In fig. 5 [42] are represented the VUV spectra for the rare gases under proton impact. The first continuum, that (at very low pressure) exhibits structure, follows immediately the resonance radiation, and the second continuum lies at longer λ. At higher pressure (a few hundred torr) the second continuum dominates the whole spectrum.

It is now well known that these continua are due to transitions taking place from the lowest excited diatomic levels (excimers) to the repulsive molecular ground state [43].

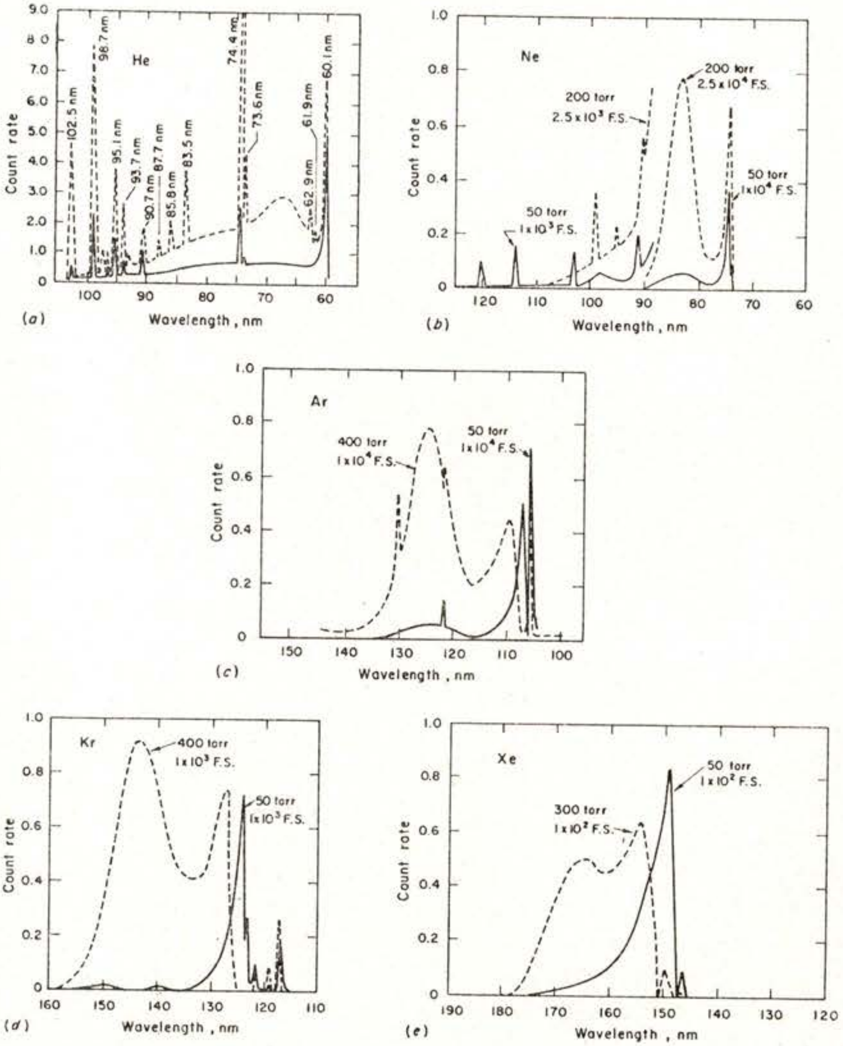

Fig. 5 — Samples of the emission spectra of various noble gases. Note the effect of impurities in He. Data taken at various fractions of full-scale (F. S.) count rates as indicated. (taken from ref. [36]). Reprinted by permission of John Wiley & Sons, Inc.

It was also observed experimentally that the spectra obtained under excitation by charged particles (α , p , e) are identical, irrespective of the kind of particle used, but they differ from the ones obtained on gas discharges [41].

In the visible and infrared, the emission observed so far is atomic in nature and attributed to cascade transitions ending at the ls levels (Paschen), the most important being the transitions $2p - 1s$ [3], [43] - [47].

Very few results regarding this spectral region have been published, and the present paper is concerned only with the VUV region, partly for the above mentioned reason but mainly because the VUV is the region potentially more interesting as most of the emission lies on this region. However, a detailed study of the visible and IR regions is essential for a complete understanding of the mechanism of radioluminescence [3].

The physical processes leading to the continuous emission are thought to be understood today, at least qualitatively; however, quantitatively they are not yet fully established and they are the subject of current investigation.

3.2 — *Electronic structure and potential curves of diatomic molecules of rare gases*

The knowledge of the electronic structure of the rare gas dimers is the clue to the understanding of most of the relaxation processes that lead the atomic ions and excited atoms to the lowest bound state of the excimers.

Although the ground state of these species is repulsive (except for a weak Van der Waals binding) [48], all rare gases form positive molecular diatomic ions reasonably stable, and by addition of one electron in a Rydberg molecular orbital, they should originate numerous molecular excited states, bound and unbound in correspondence to the molecular ion.

Potential curves for the rare gases are more or less known from the work of Mulliken, though more qualitatively than quantitatively; lately, better theoretical approximations and more experimental data have contributed to a better understanding of them [18], [25], [26], [49] - [55].

Except for He, electronic structure of rare gases is rather uniform, the main difference being the value of the principal quantum number, n, from the electrons belonging to the outer shell. Most of the systematic differences observed between the atomic spectra of these elements arise from the monotonic increase of the spin-orbital coupling as one goes from Ne to Xe (table III [31] and fig. 6 [56]) [57]; a similar behaviour is expected for the molecular states, so that potential curves for any one should be representative (qualitatively) of the ones for the other gases.

TABLE III — Some energy levels of the rare gases (eV) (from. ref. [56]).

	$^3P_2$	$^3P_1$	$^3P_0$	$^1P_1$	$^2P_{3/2}$	$^2P_{1/2}$	R_2^+
Xe	8.31	8.43	9.44	9.57	12.13	13.43	11.16
Kr	9.91	10.03	10.56	10.64	14.00	14.66	13.00
Ar	11.56	11.62	11.72	11.82	15.75	15.93	14.71
Ne	16.61	16.67	16.71	16.84	21.56	21.66	20.9
	($2\,^3S$)	($2\,^1S$)		($2\,^1P$)	(^2S)		
He	19.81	20.61		21.21	24.58		23.3

To a given pair of rare gas atoms in contact in the electronic configuration of the ground state $\ldots ns^2\, np^6$ (atomic term $^1S_0$), corresponds the electronic molecular configuration $\ldots (\sigma_g\, ns)^2\, (\sigma_u\, ns)^2\, (\sigma_g\, np)^2\, (\pi_u\, np)^4\, (\pi_g\, np)^4\, (\sigma_u\, np)^2$. This configuration should lead to a repulsive molecular state $^1\Sigma_g^+$, that represents the ground state of the rare gas molecules.

In fig. 7 [48], due to its relevance to the present work, are represented the potential curves of some excited molecular states of $Xe_2^{\star}$, precisely those curves corresponding to the electronic molecular states that dissociate to the four ls states of Paschen. They are the most relevant to the processes originating the radioluminescence of rare gases [8].

A few points deserve a comment:

1) An important characteristic of the structure of the molecular state of rare gases is the existence of two strongly attractive states

of the excimer, ${}^3\Sigma_u^+$ and ${}^1\Sigma_u^+$ lying very close together and dissociating respectively to ${}^3P_2 + {}^1S_0$ and ${}^3P_1 + {}^1S_0$. They are the lowest excited molecular states. They are practically Rydberg states originating from the R_2^+ ion core [48] [58]. The excited electron in ${}^3\Sigma_u^+$ and ${}^1\Sigma_u^+$ is loosely bound and has little effect on the molecular binding

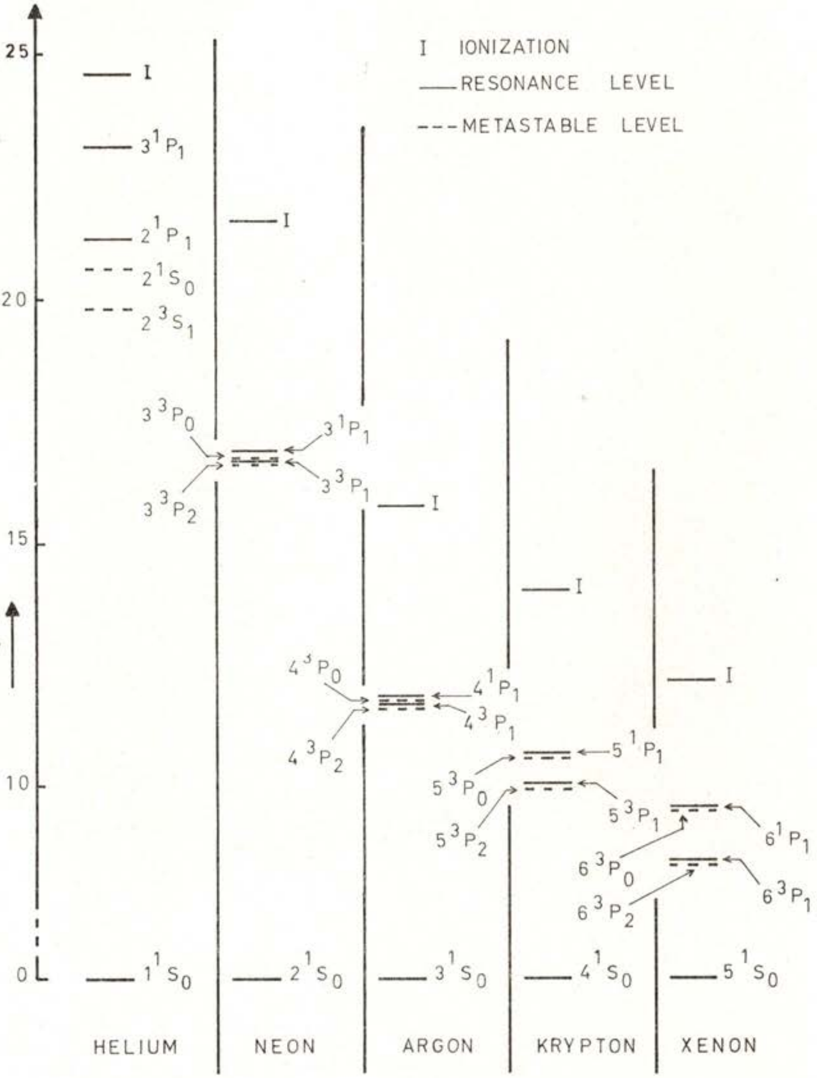

Fig. 6 — Ionization potential and lowest resonance and metastable levels of rare gases (taken from ref. [31]).

energy. Thus the general features of R_2^+ systems are expected to be repeated in various states of $R_2^\star$ with respect to binding energy, shape of the potential surface and location of the energy minimum [57]. Theoretical calculations as well as experimental results from scattering measurements [49] [52] [59] tend to confirm this expectation [50] [53] [60].

2) The molecular states $^3\Sigma_g^+$ and $^1\Sigma_g^+$ have potential curves showing small bumps or potential barriers that may eventually pre-

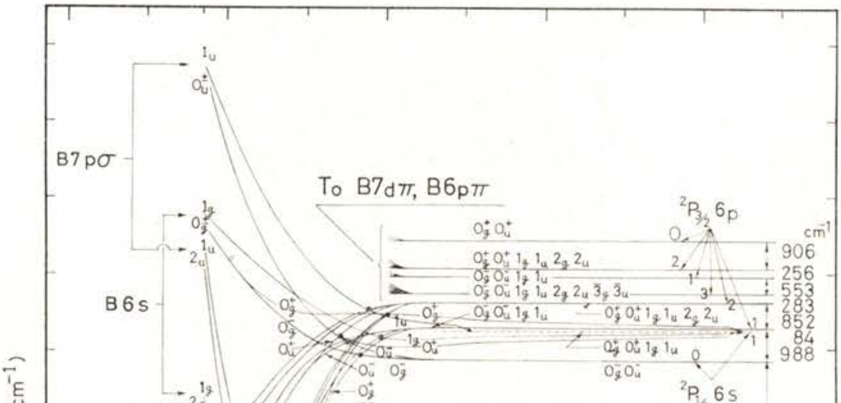

States of Molecule Ion

	$\sigma_g 5p$	$\pi_u 5p$	$\pi_g 5p$	$\sigma_u 5p$
$A^2\Sigma_u^+$	2	4	4	1
$B^2\Pi_g$	2	4	3	2
$C^2\Pi_u$	2	3	4	2
$D^2\Sigma_g^+$	1	4	4	2

Fig. 7 — Estimated potential curves for some of the lower excited states (Rydberg states) of Xe_2 (taken from ref. [48]).

vent its population by thermal collisions. They are weakly bound states, having small potential wells.

3) In every 1s state of Paschen, except at $^3P_0$, converge both attractive and repulsive potential curves; the $^3P_0$ state does not form attractive molecular states through collision with $^1S_0$ [48].

4) Both $^3\Sigma_u^+$ and $^3\Sigma_g^+$ have two substates, respectively (1_u, 0_u^-) and (1_g, 0_g^-).

5) $^1P_1$ can form, through collisions with $^1S_0$ a strongly attractive state, 0_g^+ and another less attractive state, 0_u^+, among others.

It is a well known fact that from the interaction of excited atoms with identical atoms on the ground state, continua spectra can be obtained. These are the result of a Franck Condon transition in the diatomic collision complex and are classified as recombination spectra or dissociative spectra according to the stability of the final molecular state. The VUV continua of the rare gases are dissociative continua corresponding to transitions from the excited states of the excimers to the ground state, but the transitions involved occur at internuclear distances very small, where the potential curve is purely repulsive.

According to the selection rules, the transition $^1\Sigma_u^+$ (0_u^+) → $^1\Sigma_g^+$ (0_g^+) is fully allowed, having a large oscillator strength and a small lifetime. The transition $^3\Sigma_u^+$ (1_u) → $^1\Sigma_g^+$ (0_g^+) is also allowed, although with a smaller probability, then longer radiative lifetime. The transition $^3\Sigma_u^+$ (0_u^-) → $^1\Sigma_g^+$ (0_g^+) is forbidden by the selection rules.

The states $^3\Sigma_u^+$ and $^1\Sigma_u^+$ are so close in energy and the ground state potential curve is so steep that the radiation originating in the transition from those states to the ground state appears as a unique band that cannot be spectroscopically resolved in two components. In argon, for example, according to the last theoretical calculations [52] to estimate the spin-orbital effect, the excimer $^1\Sigma_u^+$ lies $600-800$ cm^{-1} ($0.075-0.1$ eV) above $^3\Sigma_u^+$. Experimental work on the luminescence of gaseous argon following an electrical discharge [61] and excitation by α-particles [62] indicate for the separation $^1\Sigma_u^+ - {}^3\Sigma_u^+$ a value of 0.04 eV and 0.052 eV, respectively, while experimental work on solid argon [63] indicates a value of 0.03 eV. According to Jortner et al. [58] the emission spectra of argon is practically identical in the gaseous, liquid and solid phase. For xenon, Mulliken [48] [64] estimated for the energy gap ${}^1\Sigma_u^+ - {}^3\Sigma_u^+$ a value of 2000 cm^{-1} (0.24 eV), while Lorents [52] [65] calculated a value of 0.2 eV. However, recently Keto [66] estimated from experimental work a value of 0.04 – 0.08 eV for a temperature range of 200 – 300 K, in good agreement with the experimental values of 0.03 eV determined by Collier on solid xenon [67] and 0.04 ± 0.02 eV by Zimmerer also on solid xenon [63]. Though not exactly known, the energy difference of those levels is surely a small value that should not vary too much among the heaviest rare gases [65], and contributes less to the bandwidth of the emission than the slope of the repulsive potential curve. Still according to theoretical calculations, for small internuclear distances the energy difference between the 0_u^- and 1_u sublevels of the ${}^3\Sigma_u^+$ state must be very small: $Ne_2^* < 1$ cm^{-1}, $Ar_2^* < 3$ cm^{-1}, $Kr_2^* < 25$ cm^{-1}, $Xe_2^* < 80$ cm^{-1} [65]. The value in Xe_2^* agrees with other reports [68]. So, the two emissions ${}^3\Sigma_u^+ - {}^1\Sigma_g^+$ and ${}^1\Sigma_u^+ - {}^1\Sigma_g^+$ cannot be distinguished on an energy base, but they should be distinguishable on a time base, as the radiative lifetimes of both transitions are very different (ns and μs) and this leads to two components in the time decay curves, as experimentally observed.

3.3 — *Ion recombination.*
Creation and evolution of molecular ions

The ions formed upon the passage of the ionizing radiation through a material [20] [35] [69] have a certain probability of being neutralized by recombination from various processes, from which we stress:

3.3.1 — *Radiative recombination*

It is a reaction of the kind

$$e + X^+ \rightarrow X' + h\nu$$

The recombination process is described by a recombination coefficient α_e, defined from the equation

$$d n_e / dt = - \alpha_e n_e n_+$$

where n_+ is the ion density and n_e is the electron density.

When the state reached is the ground state, the process is just the reverse of photoionization and the value of α_e can then be deduced. Theoretical calculations (mainly for H) show that cross sections are small, about 10^{-19} cm^2, leading to recombination coefficients $\alpha_e - 10^{-12}$ cm^3 s^{-1} [34] [35], so that this process is negligible under the usual experimental conditions ($n_e \sim 10^{11}$ cm^{-3}). It is however very important under special conditions, for example in gas nebulae.

3.3.2 — *Recombination ion-electron with participation of a neutral atom*

It is a reaction of the kind

$$X^+ + e + X \rightarrow X + X$$

or

$$X^+ + e + X \rightarrow X^\star + X \rightarrow X + X + h\nu$$

or

$$X^+ + e + Y \rightarrow X + Y$$

In this process, the excess of internal energy of the recombination collision is removed by a neutral atom or by a molecule of the same or of other kind. At very high pressures, the probability of the presence of a neutral atom in the vicinity of the ion-electron system is large enough so as to make this process important, and its recombination coefficient is larger than the preceeding one. This collision is treated in detail in ref. [69]. Defining the recombination coefficient α for this process from the equation

$$dn_+ / dt = -\alpha\, n_e\, n_+$$

α is now a function of the pressure p. Representative values of α are of the order of 10^{-11} p cm^3 s^{-1} for He [35] reaching a saturation value at a pressure of $\sim 10^4$ torr [69]. For argon at 1 atm, $\alpha \sim 10^{-8}$ cm^3 s^{-1} [34]. If we calculate the fraction of ions neutralized after a period of 10^{-6} s, a value of $\sim 10^{-3}$ is obtained [34]. So, the number of excited atoms formed from the recombination ion-electron upon ternary collisions is also negligible for argon and similarly for the other rare gases except at very high pressures and electronic densities.

3.3.3 — *Dissociative recombination*

It is a perfectly well known fact that at very low pressures the ions present in a gas are monoatomic, but at high and even moderate pressures the ions that recombine are mostly from the molecular type X_2^+, formed upon a three-body collision of the type

$$X^+ + 2X \rightarrow X_2^+ + X .$$

On the other hand, photoexcitation of rare gases for atomic levels above a threshold result in formation of the diatomic ion (section 3.4.5) and the appearance potential of the molecular ion is lower by about $1-2$ eV than the one of the corresponding atomic ions (table III [56]). These molecular ions participate then in recombination reactions of the kind

$X_2^+ + e + e \rightarrow X_2^\star + e$ in a strongly ionized plasma

$X_2^+ + e + X \rightarrow X_2^\star + X$ in a dense gas

$X_2^+ + e \rightarrow (X_2^\star)$ unstable $\rightarrow X^\star + X$ dissociative recombination

The excited atoms produced by dissociative recombination can also form excited molecules. The emission of these molecules is the cause of the recombination component of the scintillation light experimentally observed [41] (section 3.1). The dissociative recombination has been recognized since several years as being capable of taking place at a much higher speed than the recombination processes considered so far. It represents probably the main contribution for the recombination rates measured in weakly ionized gases and in the upper atmosphere. The rate equation for this process is

$$\frac{1}{n_+} \frac{dn_+}{dt} = - K N^2$$

K being the rate constant, n_+ the density of X^+ and N the density of atoms X.

Values of K for the various rare gases have been obtained by several processes. With a typical value of 10^{-31} $cm^6\,s^{-1}$ [70] a positive atomic ion is converted to a molecular ion within a time of ~ 10^{-8} s at a pressure of 1 atm. For argon, $K = 2 \times 10^{-31}$ cm^6 s^{-1} [71], and the reaction is efficient even at low pressures ($p > 10$ torr) [45]. The fast conversion of atomic ions to molecular ions is followed by the process of dissociative recombination [72]. The rate equation for this process is

$$\frac{1}{N_+} \frac{dN_+}{dt} = - \alpha n_e$$

N_+ being the density of X_2^+, α the recombination coefficient and n_e the electronic density. References [35] and [72] contain tables of experimental values of α for the rare gases. For a typical value of 10^{-7} cm^3 s^{-1} and an electronic density of 10^{11} cm^{-3}, the rate of recombination for a molecular positive ion is 10^4 s^{-1} [36]. An experimental value of ~ 10^{-5} s is indicated [38] for the recombination of a thermalized electron and an ion in xenon for a range of pressures of $5 - 50$ atm. From the exposed, it is to be expected that when a heavy charged particle creates a large density of ion-pairs in a noble gas at 1 atm pressure, the ions X^+ are converted to X_2^+ in about 10^{-8} s. A much longer time ($10^{-4} - 10^{-5}$ s) is necessary for the molecular ion to recombine with an electron in a process of dissociative recombination. This process becomes very important at high values of pressure and n_e, but it is probably unimportant at low pressure (< 1 atm) (section 3.1).

The mechanism of dissociative recombination

$$X_2^+ + e \rightarrow (X_2^\star) \text{ unstable} \rightarrow X^\star + X + \text{kinetic energy}$$

is well illustrated in the work of Bardsley and Biondi [72]. This process is fast only if the final potential curve crosses the one of the diatomic ion near its minimum. This is the case for the rare gases other than He [36]. Fig. 8 shows some relevant potential curves for Ar_2 [52] that illustrate the proposed mechanism [72]. The excited atomic states preferentially populated are the 2p states (Paschen) that in Ar correspond to the $3p^5\,4p$ states [73] [74].

The dissociation can be followed by emission of atomic and/or delayed molecular radiation. For He, according to Mulliken, the molecular potential curves resulting from the combination of a ground state atom and an excited atom lie bellow the ones belonging to the diatomic ion He_2^+, so that they do not provide a dissociative pathway. The excited molecules formed upon radiative combination can afterwards emit radiation for lower states. This cascade radiation has indeed been observed experimentally [36].

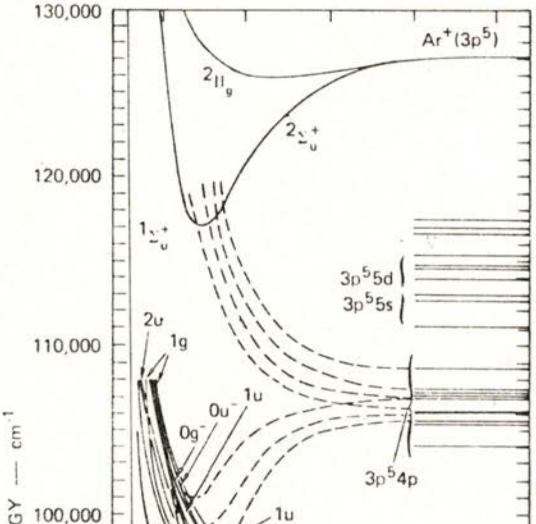

Fig. 8 — Argon intermolecular potential curves (taken from ref. [52]).

3.4 — *Deexcitation of excited atomic states*

The primary activated states created in the sequence of the passage of a charged particle through a gas evolve to the excitation levels responsible for the light emission following pathways that depend on the nature of the radiative and collisional processes that take place. It should be stressed that the levels involved in these processes can be obtained through direct excitation, or as a result of cascades or in the sequence of collisions, or through ion-electron recombination, and this makes the kinetics of the process and its dependence on temperature and pressure very complicated.

The main pathways for deexcitation of excited atomic states are summarized below. Numerical values are indicated for argon that is representative of the remaining heavy rare gases.

3.4.1 — *Radiative deexcitation*

For optical and resonant states emission can take place respectively through cascading or directly to the ground state:

$$X^{\star} \rightarrow X + h\nu$$

$$X^{\star} \rightarrow X^{\star\prime} + h\nu'$$

$$X^{\star\prime} \rightarrow X + h\nu''$$

The resonant emission occurs both from ${}^1P_1$, and ${}^3P_1$ to S_0, but it is strongly reabsorved and reemitted [75] (radiation retention) leading to an increase in the duration of these excited states that may last a few μs (as the metastables ${}^3P_2$ and ${}^3P_0$) though its radiative lifetime is of a few nanoseconds [76]. They are then able to participate in collisional deactivation processes.

Radiation retention has been treated by Holstein [75]. It depends both on pressure and geometry of the medium. For argon, for example, for a 1-2 cm diameter cell, radiation retention is already well noticeable at pressures < 10 torr [36]. For pressures ~ 400 torr, the transmitted resonance radiation is already negligible due both to radiation retention and collisional competition [77].

The most important cascade transitions for the rare gases are the 2p – 1s. Some of these are tabulated for Ar in ref. [45] together with its wavelength and oscillator strength, when known. Lifetimes for these transitions are of the order of 20 – 30 ns [78] and they lie, as for the other rare gases, in the infrared, their extreme values of λ being 6677 and 10470 Å. They are easily observed at low pressures, but they are inhibited even at medium pressures through competition with collisional processes. Arai and Firestone [46] still observe the 2p – 1s emission in argon at 1031 torr, though atomic emission in the visible, IR and UV represents a negligible fraction of the total excitation [33]. According to Bennett et al [79] for argon at 1 atm 90% of the total emission is centered in the second continuum.

The 3p – 1s transitions, with lifetimes of 100 – 200 ns [45], lie in the visible, but they are observed only at low pressures. For Ar, λ situates between 3900 and 4700 Å. They are clearly observed [43] at 200 torr.

Above 10 torr all atomic emission from states higher than the appearance potential of the diatomic ion disappear [8], [45]-[47] due to the inhibition of the process by the known Hornbeck-Molnar effect [44] [80] (section 3.4.5).

3.4.2 — *Deexcitation by diffusion and collision with the container's walls*

$$X_m^* \rightarrow X$$

This is the dominant process for metastable states at low pressures. For $p > 100$ torr, collisional processes are already dominant [81].

3.4.3 — *Collisional transfer of electronic energy*

It is a reaction of the kind

$$X_1^* + X_2 \rightarrow X_1 + X_2^* \qquad ,$$

X_1 and X_2 being the same atomic species.

This process is also called a second kind collision. Its cross section σ depends on the energy difference ΔE between X_1^* and

$X_2^\star$. For the 1s states of Ar, $\Delta E \sim 0.1$ eV, $\sigma \sim 10^{-20} - 10^{-21}$ cm^2, so for $p = 1$ atm the frequency of collisions taking place (per particle) is $\sim 10^3 - 10^4$ s^{-1} [30]. These collisions tend to redistribute the energy of the primary levels among the electronic levels of identical energy, so that the most populated tend to be those of lower energy. However, this coefficient of 'collisional mixture' is small.

For higher levels, for example the 2s levels, $\Delta E \sim kT$ (0.025 eV at room temperature), $\sigma \sim 10^{-15}$ cm^2 [30], so for $p = 1$ atm the number of collisions per second is $2 \cdot 10^9$ and the mixture is efficient [34].

3.4.4 — *Formation of excimers through three-body collisions*

$$X^\star + 2X \rightarrow X_2^\star + X$$

$$X_2^\star \rightarrow X + X + h\nu$$

This process is the dominant one even at relatively low pressures (~ 50 torr), and is more important than second kind collision. Typical values of rate constants for these reactions are $\sim 10^{-32}$ cm^6 . s^{-1} [34] so that at 1 atm the frequency of collision is $\sim 7 \times 10^6$ s^{-1}, rather higher than for binary processes.

3.4.5 — *Hornbeck-Molnar reactions — Associative ionization processes*

$$X^{\star\star} + X \rightarrow X_2^+ + e$$

Any excited atom whose energy lies between the appearance potential of the molecular ions and the ionization potential of the atom is susceptible of creating, through binary collisions with neutral atoms, a molecular ion [80]. For every atom there is a threshold state; for argon it is the state $3p^5 4d$, and it is observed that every excited state of higher energy can originate the molecular ion [82]. The threshold states for the rare gases are summarized in reference [36] together with the threshold energies. A very recent determination of the appearance potential of Ar_2^+ via associative ionization indicates the value 14.6 ± 0.2 eV [83].

The mechanism of the Hornbeck-Molnar reactions is well understood from the potential curves. However, it should be noted that the efficiency of Hornbeck-Molnar processes is not unity, as there is experimental evidence [82] that it competes with a reaction of the type

$$A^{**} + A \rightarrow A^{*} + A$$

Fig. 9 summarizes all the deexcitation processes mentioned above in a kinetic scheme. Their relative importance depends on the pressure and electronic density conditions, but the origin of the atomic lines and of the continua of the rare gases emission in the VUV is qualitatively understood.

Of course, additional processes of deexcitation occur in the presence of impurities or mixtures of rare gases. These include energy transfer processes [36] [43] [84] [85], formation of mixed excimers or mixed diatomic ions [83], [85] - [88] but this field is out of the scope of the present work.

4 — MECHANISM OF LUMINESCENCE

In the establishment of the mechanisms of luminescence it is particularly relevant the study of the time dependence of the emission spectrum in a large range of pressure. This study, individually made for every line and band of the emission spectrum, would give valuable information for the establishment of the atomic precursors of the continua emission, as well as for the pathways of deexcitation and cross sections for these processes.

Of course, the evolution of the atomic states initially excited will depend strongly on the pressure through the collisional processes taking place. It is common practice to divide kinetic studies into two classes: the low pressure region ($\leqslant 1$ atm) and the high pressure region (> 1 atm). The last one, where collisional processes are very fast, is the region of potential interest for lasers. Besides, two further classes can be distinguished, according to the density of deposition of energy or the density of excitation and the resulting electronic density. For low electronic densities ($n_e \leqslant 10^{10}$ cm^{-3}) the ion-electron recombination processes are slow relative to the rates of formation and relaxation of the excimers, and as a result only processes originating at neutral excited atoms are interesting. For high electronic densities ($n_e \gg 10^{14}$ cm^{-3}) not only is recombination a fast process but the thermalized electrons play an important role in the relaxation of the excitation of the excimers levels; electronic collisions are an important process of mixture of excited states.

For pressures up to 10^3 torr, excitation by electrons, protons and alpha particles is usually under conditions of low electronic density.

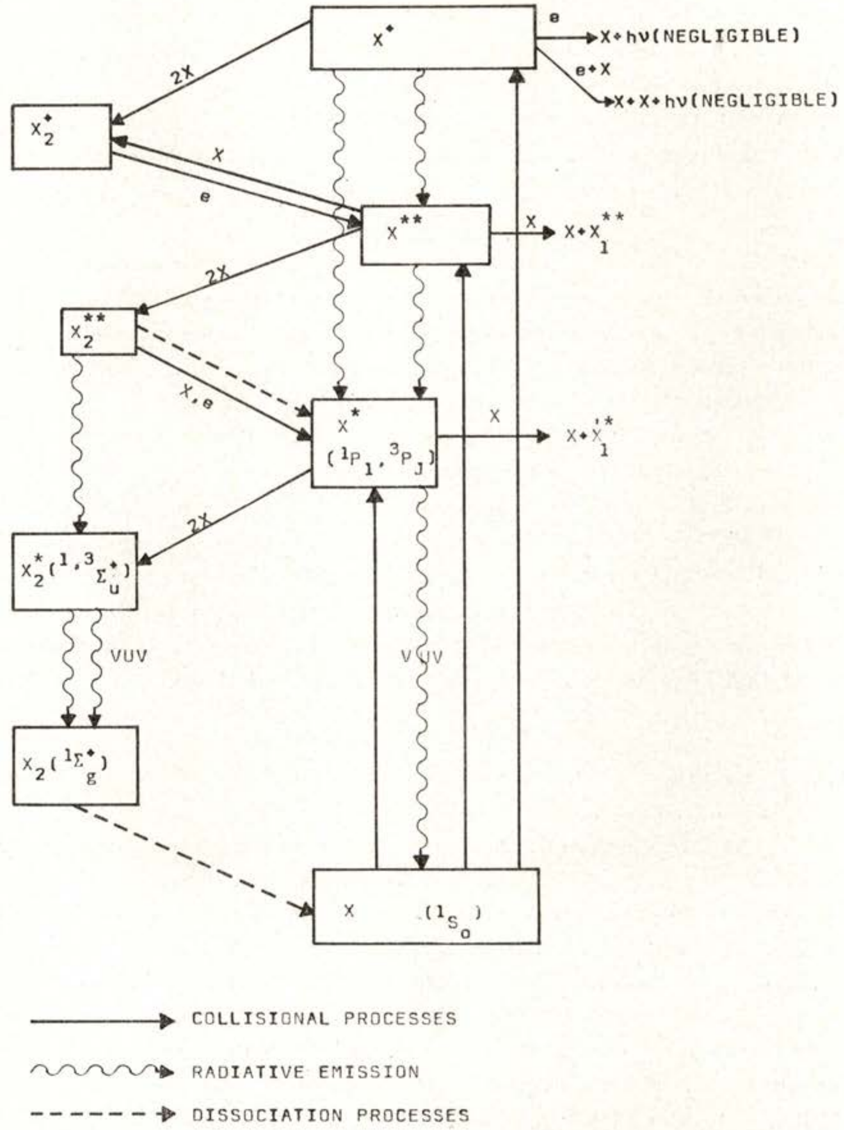

Fig. 9 — Schematic diagram of the deexcitation processes in a rare gas following excitation by charged particles impact.

This is the situation we shall deal with firstly. At high pressures, there are measurements made in conditions of both high and low electronic density, which we shall consider afterwards.

For low pressures, there is information for every rare gas, though a detailed and exact mechanism for the formation and decay of a large variety of atomic and molecular excited species is still to be established. The behaviour of the heavier rare gases is identical, so we shall take argon as representative of all the others.

Argon presents in the VUV region a sharp resonance line at 1048 Å, the first continuum originating apparently at the other resonance line at 1067 Å, and a second continuum, broad, roughly gaussian, centered at 1270 Å.

At very low pressures (< 10 torr) only the two resonance lines are observed, but at about 25 torr the two continua emissions are well noticeable [8] [89]. As the pressure increases, the second continuum tends to dominate the whole spectrum, this being the situation at a few hundred torr.

Work done by Michaelson and Smith [53] at very low pressures (4 - 20 torr) and low temperatures ($125\ \mathrm{K} < \mathrm{T} < 200\ \mathrm{K}$), showed that the first continuum has structure and begins at 1074 Å, the energy of the forbidden transition ${}^3P_2 - {}^1S_0$. Recently, Tanaka et al [54] [55] studied the emission spectra of the argon dimer in the pressure range 0.1 - 70 torr. They observed, in addition to the second continuum, four emission band systems. According to them, the so called first continuum could be a combination of these.

4.1 — *The origin of the two continua*

It has been generally accepted, according to a proposition by Mulliken based on theoretical considerations, that the fist continuum corresponds to transitions taking place from the higher vibrational levels of ${}^1\Sigma_u^+$ and ${}^3\Sigma_u^+$, the molecular states related to the lowest atomic states ${}^3P_1$ and ${}^3P_2$, while the second continuum takes place from the vibrationally relaxed level ($\nu = 0$) of those molecular states to the same repulsive ground state ${}^1\Sigma_g^+$ [43]. The transitions from the upper vibrational levels occur mainly near the classical turning point on the attractive branch of the potential curve [54]. However, according to Tanaka et al [54] [55], three of the four observed emission band systems in the region of the first continuum could be attributed to transitions from $^1\Sigma_u^+$, $^3\Sigma_u^+$ and B 5 p σ (0_u^+) to the repulsive ground state, while the origin of the fourth one is still unknown. This being so, the origin of the first continuum is not clear at this time [54].

Table IV lists some experimental values of lifetimes for both $^1\Sigma_u^+$ and $^3\Sigma_u^+$ [52].

TABLE IV — Radiative lifetimes of excimer states (mainly taken from ref. [52])

Excimer	$^1\Sigma_u$ (ns)	$^3\Sigma_u$ (μs)	Ref.
Ne_2*	—	5.1	[7]
	2.8	11.9	[107]
	—	12 ± 6	[65]
	—	6.62	[8]
Ar_2*	—	2.8	[41]
	—	3.7	[92]
	4.2 ± 0.1	3.2 ± 0.3	[98]
	—	4.0 ± 2.0	[65]
	—	3.22	[8]
Kr_2*	—	1.7	[92]
	—	0.3	[108]
	—	0.36 ± 0.16	[65]
	—	0.35	[8]
Xe_2*	5.5 ± 1.0	0.096 ± 0.005	[98]
	—	0.140 ± 0.05	[65]
	6.22 ± 0.80	0.100 ± 0.002	[66]

4.2 — *Atomic precursors of the excimers*

4.2.1 — *Low pressure conditions ($\leqslant$ 1 atm)*

Although it is generally accepted today that both continua have their origin at $^1\Sigma_u^+$ and $^3\Sigma_u^+$, and experimental values of the radiative lifetimes of these states are known with a reasonable degree of agreement, there are still some doubts as to the mechanism of their formation, i.e., on their atomic precursors and its evolution to those molecular states. There are nevertheless a set of experimental observations that, together with theoretical considerations, allow a few conclusions to be drawn, forming a good support for the elaboration of a plausible mechanism of evolution of the atomic precursors of the radiative excimers, as summarized in fig. 10. This table deserves a few comments regarding the participation of the four 1s levels:

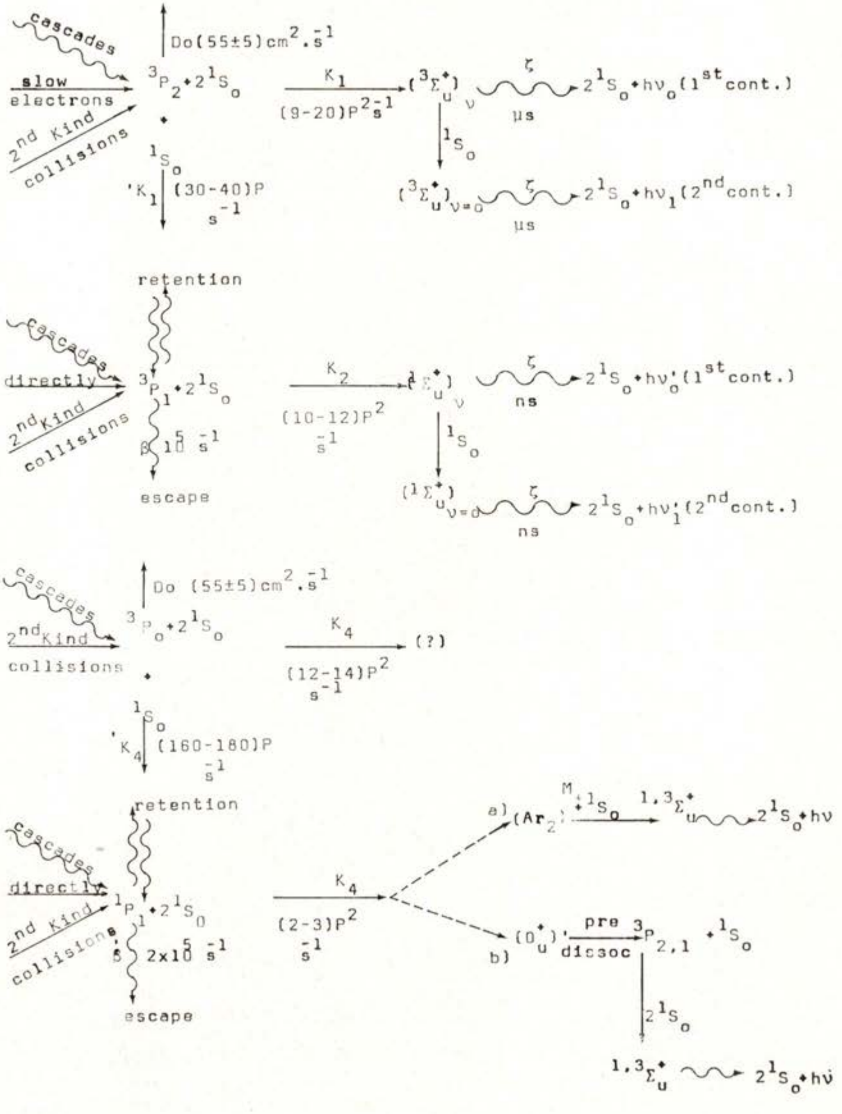

Fig. 10 — Schematic diagram of the creation of the lowest excited states of rare gases after charged particles impact and its evolution to the radiative levels of the excimer. Numerical values of rate constants are indicated for argon. 'Do' is the diffusion coefficient. Remaining symbols as refered in text.

1) Participation of $^3P_2$

a) Theoretical considerations show that $^3P_2$ is the direct atomic precursor of $^3\Sigma_u^+$, whose dissociation limit is $^3P_2 + {}^1S_0$; $^3\Sigma_u^+$ can be formed upon ternary collisions $^3P_2 + 2\ {}^1S_0$.

Experimental observations show that the evolution of the metastable state $^3P_2$ takes place indeed by a mechanism involving binary and ternary collisions. Every experimental observation agrees in this point, although the values of the rate constants are widely different as shown in table V. Ternary collisions are dominant even at low pressures.

b) Time dependent measurements made in the sequence of electrical discharges that populate preferentially $^3P_2$ point to this state as being the main precursor of the radiative excimers, as the decay rate of the continua is consistent with the rate of disappearance of $^3P_2$, i.e., the rate of production of $^3\Sigma_u^+$ agrees well with the rate of disappearance of $^3P_2$ at low pressures (up to 50 torr) [41], [66], [90] - [93]. According to Michaelson and Smith [53] the first continuum decays at a rate comparable to that of $^3P_2$. For $p > 50$ torr, three body collisions involving the other atomic states feeding the excimer levels become increasingly important [93], and that relationship is blurred.

c) On excitation under fast heavy charged particles, $^3P_2$ is not directly excited. Its importance under these conditions is certainly much lower than under discharges, where it is the most populated of the 1s states due to the high proportion of slow electrons, but its population cannot nevertheless be ignored as $^3P_2$ can be populated by three main processes:

- on the sequence of radiative cascades from the excited states 2p (and in a less extent from 3p),
- collisions of the second kind,
- collisions with slow electrons

2) Participation of $^3P_1$

Theoretical considerations show that $^3P_1$ is the direct atomic precursor of $^1\Sigma_u^+$, whose dissociation limit is $^3P_1 + {}^1S_0$; $^1\Sigma_u^+$ can be

TABLE V — Collisional rate constants for argon

Reaction	Experimental values of K									
$^3P_2 + 2\,^1S_0 \xrightarrow{K_1}$ Products	K_1	9	13.5	20 ± 2	7.6 ± 0.5	8.3	18.0 ± 0.2	9	20	5.2
	$(\text{torr}^{-2}\ s^{-1})$									
	Ref.	[113]	[114]	[91]	[115] [116]	92]	[93]	[117]	[118]	[94]
$^3P_2 + {}^1S_0 \xrightarrow{K'_1}$ Products	K'_1	40		31 ± 6	29		45 ± 5	60	78	
	$(\text{torr}^{-1}\ s^{-1})$									
	Ref.	[113]		[91]	[115] [116]		[93]	[114] [119]	[120]	
$^3P_1 + 2\,^1S_0 \xrightarrow{K_2}$ Products	K_2	10.6	12.5	10	3.5	21.4				
	$(\text{torr}^{-2}\ s^{-1})$									
	Ref.	[94]	[89]	[93]	[98]	[118]				
$^3P_0 + 2\,^1S_0 \xrightarrow{K_3}$ Products	K_3	12.0								
	$(\text{torr}^{-2}\ s^{-1})$									
	Ref.	[91]								
$^3P_0 + {}^1S_0 \xrightarrow{K'_3}$ Products	K'_3	160								
	$(\text{torr}^{-1}\ s^{-1})$									
	Ref.	[91]								
$^1P_1 + 2\,^1S_0 \xrightarrow{K_4}$ Products	K_4	2.20 ± 0.05		11.4						
	$(\text{torr}^{-2}\ s^{-1})$									
	Ref.	[41] [121]		[118]						

$K\ (\text{cm}^3\,s^{-1}) = K'\ (\text{torr}^{-1}\,s^{-1}) \,.\, 760/L$, $K\ (\text{cm}^6\,s^{-1}) = K'\ (\text{torr}^{-2}\,s^{-1}) \,.\, (760/L)^2$, L = Loschmidt number (2.6871×10^{19} at cm^{-3})

formed upon ternary collisions $^3P_1 + 2\ ^1S_0$, that compete with the resonance emission for the deexcitation of $^3P_1$. Experimental observations confirm that the deexcitation of $^3P_1$ occurs indeed by radiative emission and by ternary collisions [41] [93] [94].

3) Participation of $^3P_0$

According to Mulliken, $^3P_0$ does not form, upon collision, stable molecular states, as it forms only 0_g^- and 0_u^-. However, its destruction, occurs also partly by two- and three-body collisions [91]. Its eventual participation in the process is not clear and it has not been included in a kinetic scheme so far, as under swift charged particle excitation its importance is much less than that of $^3P_2$ due to its much smaller population, although recent work [95] tends to show that $^3P_0$ is more populated than it is generally supposed to be.

4) Participation of $^1P_1$

The excited states $^1P_1$, bound to the ground state by the largest oscillator strength are the most populated under fast charged particle excitation. Its deexcitation must include some form of emission. The intensity of its resonant emission decreases strongly with increasing pressure, and this decrease is accompanied by an increase of the continuum intensity [36]. There is a qualitative relation between the intensities of both emissions, well revealed in the spectra of fig. 5. Though $^1P_1$ does not form directly $^{1,3}\Sigma_u^+$ upon collision with ground state atoms, there are several reasons that point out to considering $^1P_1$ as an important precursor of the continuous emission:

a) Fig. 11 [41] shows the time evolution of the second continuum of argon at several pressures, as well as the resonant radiation of $^1P_1$ under excitation with charged particles. Regarding the continuum it is interesting to remark that its intensity goes on increasing after the excitation pulse has ended and the peak is reached only about 0.3-10 μs after the end of the excitation pulse. This time delay decreases with increasing pressure. It can be seen as well that the decay of the resonance radiation takes place within the rising time of the second continuum, suggesting [41] the possibility of that atomic state being one of the contributors to the formation of the continuum. This suggestion is corroborated by the observation that the time interval necessary to reach the peak of the 1250 Å continuum decreases with increasing pressure, and this may relate to the decreasing lifetime of $^1P_1$ at high pressures. However, the time delay of the peak emission seems to suggest that this does not occur only through Franck-Condon emission, but it also depends on a process of collision that transfers energy from a state initially excited to an intermediate state [36]. For $p > 3$ atm the rising time of the second continuum cannot be determined as it is of the same order of the excitation pulse.

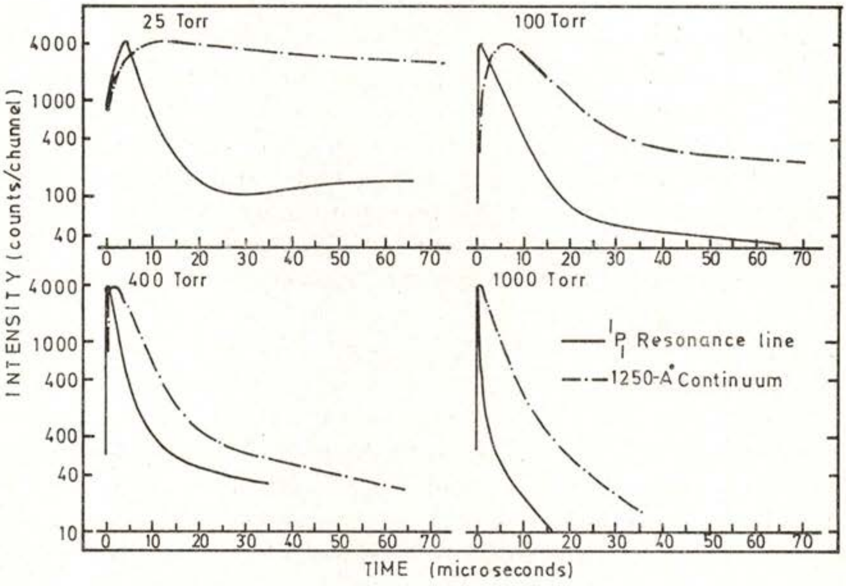

Fig. 11 — Comparison of time dependence of the $^1P_1$ resonance level and the 1250 Å continuum from 25 to 1000 torr.

——— $^1P_1$ resonance line

-·-·-· 1250 Å continuum

25 torr data taken with 0.4 μs excitation; 100 to 1000 torr data taken with 0.5 μs excitation (from ref. [41]).

b) $^1P_1$ does not form, upon direct collision with $^1S_0$, the radiative states $^{1,3}\Sigma_u^+$ of the excimer [48]. However, it can form a 0_u^+ state, almost unstable, having a small potential well [36]. This state could radiate to the ground state ${}^1\Sigma_g^+$ through an allowed transition whose wavelength should be shorter than ${}^3P_2$ - ${}^1S_0$. Emission band system III from Tanaka et al [54] [55] beginning at 1048 Å could possibly account for it. However, most of the VUV continuous emission comes from the ${}^{1,3}\Sigma_u^+$ radiative states [36]. This means that, if the 0_u^+ state is formed upon collision, it must also decay in another way. Two channels have been suggested to account for the participation of ${}^1P_1$ in the formation of radiative excimers, as shown schematically in fig. 10: channel a) proposed by Hurst et al [36] consists in the formation of a metastable molecule that further collisions would convert to a radiative molecule. This scheme does not seem to be corroborated from the potential curves. Besides, the rising time of the second continuum is too fast to occur via a metastable molecule. Scheme b) [36] [96], consistent with the potential curves, is more likely to describe the correct mechanism. The 0_u^+ state formed from ${}^1P_1$ can predissociate through potential curve crossing to the atomic levels ${}^3P_{1,2}$, this predissociation being followed by the formation of a new molecule. This mechanism could explain (at least qualitatively) the observed behaviour in the time evolution of the continua and of ${}^1P_1$ and its dependence on pressure, but it still awaits experimental confirmation.

Besides the channels indicated in fig. 10, that must contain the main modes of formation of radiative excimers, others have been suggested starting from ${}^3P_2$ and ${}^1P_1$. Some of these are indicated in fig. 12. However, it must be stressed that they all await experimental confirmation, that must include measurements in the infrared region that, to our knowledge, have not been tried so far.

These mechanisms deserve a few comments:

1) Measurements made under certain conditions following electrical discharges in rare gases seem to suggest that ${}^3P_2$ could be related to the continuous emission originating from ${}^1\Sigma_u^+$: if this suggestion is correct, mechanism 1 in fig. 12 could explain it; ${}^3P_2$ does not form ${}^1\Sigma_u^+$ upon direct collision but it could form this state from an intermediate state. Through the collision, a molecular state dissociating to ${}^3P_2 + {}^1S_0$ could be formed and upon potential curve crossing it could go to a high vibrational level of ${}^1\Sigma_u^+$, the radiative state [53]. This intermediate state could be the ${}^3\Sigma_g^+$ state. The presence of a third body could remove symmetry restrictions. Tanaka and Yoshino [10] studied the higher vibrational levels of ${}^3\Sigma_u^+$ and

$^1\Sigma_u^+$ and their results indicate that there is a vibrational level of $^1\Sigma_u^+$ only 14 cm^{-1} above the dissociation limit $^3P_2 + {}^1S_0$.

2) The second channel in fig. 12 suggests another way of participation of $^1P_1$ that still needs experimental confirmation. To our knowledge, the infrared studies that it involves have not been done so far.

$$1)\quad {}^3P_2 + {}^1S_0\ (+\,{}^1S_0) \longrightarrow {}^3\Sigma_g^+\ (1g, \bar{0}g) \longrightarrow {}^1\Sigma_u^+\ (0_u^+) \overset{\nu\ \mathrm{VUV}}{\rightsquigarrow} 2\,{}^1S_0 + h$$

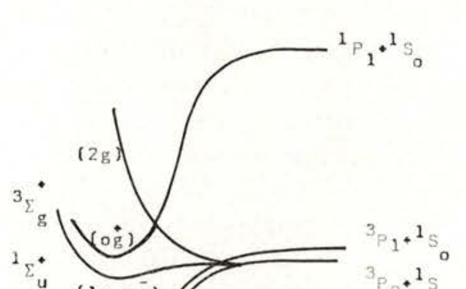

$$2)\quad {}^1P_1 + 2\,{}^1S_0 \longrightarrow 0g^+ \underset{\lambda \sim 10^4 A^0}{\overset{\mathrm{I.R.}}{\rightsquigarrow}} {}^1\Sigma_u^+\ (0_u^+) \overset{\mathrm{VUV}}{\rightsquigarrow} 2\,{}^1S_0 + h\nu$$

Fig. 12 — Additional pathways of formation of the $^1\Sigma_u^+$ radiative level.

It must be emphasized that the analysis of the experimental results including all possible precursors, or at least $^3P_1$, $^3P_2$, $^1P_1$ has not been attempted so far, and it is a task calling for urgent realization. The analysis done by Hurst et al [41] (including only $^3P_2$ and $^1P_1$ via channel a)) and that of Mortier et al [92] [97] (including $^3P_2$ and $^3P_1$) cannot be considered conclusive.

4.2.2 — *High pressure conditions* (>1 *atm*)

At high pressure, the high collision frequency establishes a vibrational relaxation in a short time relative to the radiative lifetime of the excited states. The only emission to be observed is the second continuum, as expected. Formation of excimers through ternary collisions is also very fast relatively to the radiative decay of the excited atoms.

4.2.2.1 — *Low electronic density* ($n_e < 10^{10}\ cm^{-3}$)

Fig. 13 summarizes the dominant reactions in the system under these conditions. The kinetics of the second continuum emission is simple and well represented by the equations

$$X^* + 2X \rightarrow X_2^* + X$$

$$X_2^* \rightarrow 2X + h\nu$$

Relevant work is due to Keto et al [66] [98] under electron impact, for 1 atm $< p <$ 32 atm. From the analysis of the rising and decay of the radiation following an excitation pulse, the rate constants were obtained. For argon they are displayed on fig. 13. The two excimers radiate independently, so their collisional mixture is negligible. An upper limit for the cross section of the reaction

$${}^1\Sigma_u^+ + Ar \rightarrow {}^3\Sigma_u^+ + Ar$$

was established as $6.10^{-18}\ cm^2$

4.2.2.2. — *High electronic density* ($n_e > 10^{14}\ cm^{-3}$)

This situation has been treated in great detail by Lorents [52] [65]. The main processes taking place are summarized in fig. 14. The electronic density is high and the recombination ion-electron takes place at a rate comparable to the kinetics of neutral species and is an important source of excited atoms. Under the conditions stated, all initial ionization and excitation decay very rapidly to the levels of the excimers and the system can radiate most of the available energy in a very short time.

As Lorents points out, reactions involving collision of two excited species (either dimeric or monoatomic) or absorption of the

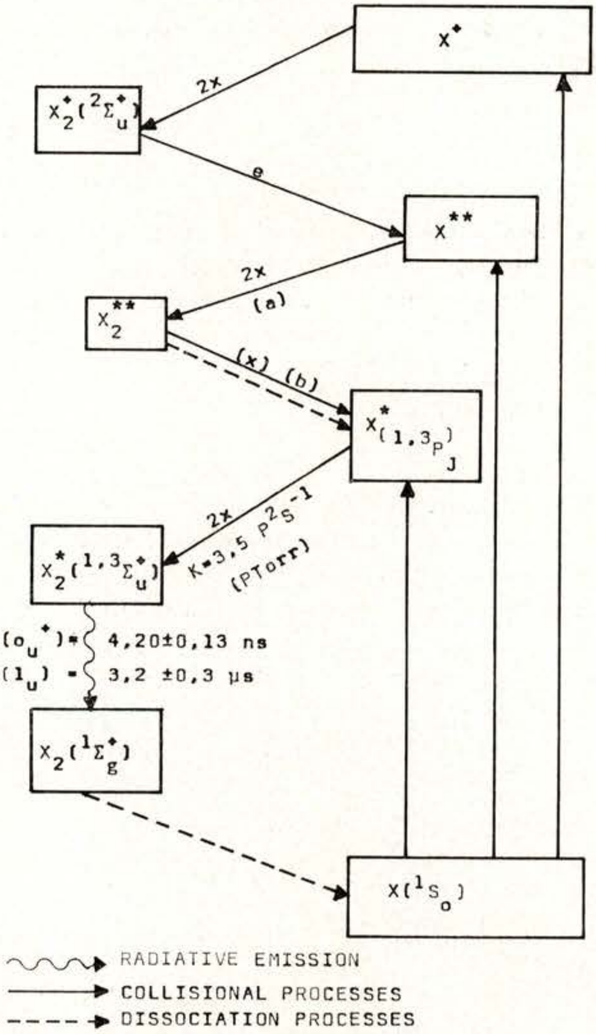

Fig. 13 — Schematic diagram of the collision kinetics for dense rare gases at low electronic densities ($p > 1$ atm; $n_e \lesssim 10^{10}$ cm^{-3}) following charged particles impact. Numerical values of rates constants are indicated for argon.

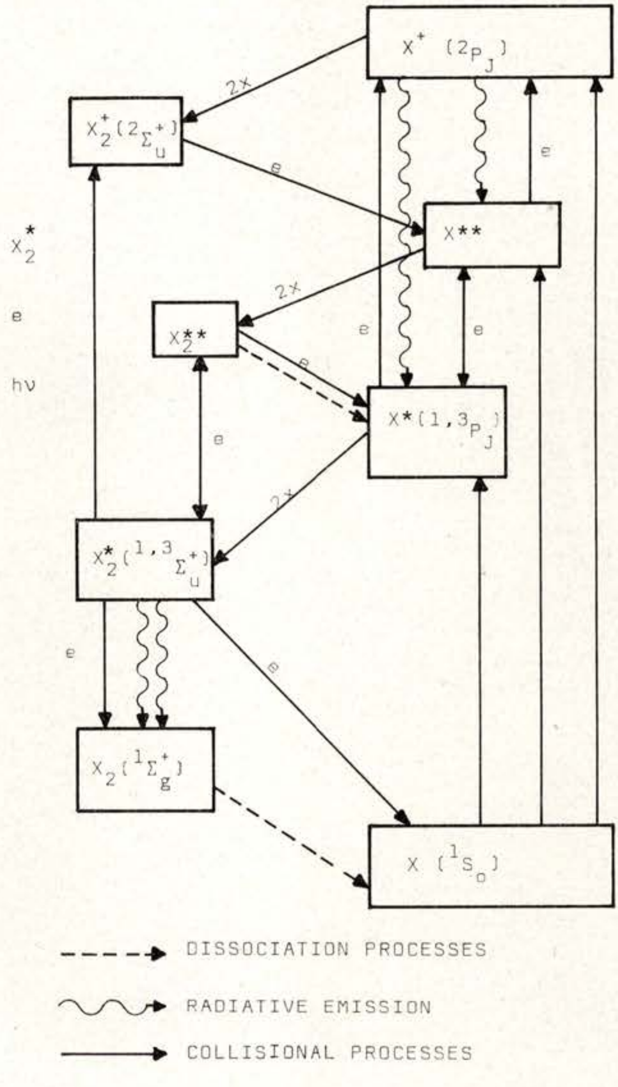

Fig. 14 — Schematic diagram of collision kinetics for dense rare gases at high electronic densities ($p > 1$ atm; $n_e > 10^{14}$ cm^{-3}) following electron impact.

excimer radiation by an excited atom or excimer resulting in ion-pair formation may be significant. Rate constants estimated for some of these reactions are indicated in table VI.

TABLE VI — Rate constants for some reactions in argon and xenon

Reaction	Ar	Ref.	Xe	Ref.
$X^{\star} + 2X \rightarrow X_2^{\star} + X$	$^3P_2$ $(1.6 - 0.5) \times 10^{-32}$ cm^6 s^{-1}	See Table V	4×10^{-32} cm^6 s^{-1}	[67]
	$^3P_1$ $(1.7 - 0.3) \times 10^{-32}$ cm^6 s^{-1}		$\sim 5 \times 10^{-32}$ cm^6 s^{-1}	[65]
	$^3P_0$ 1.0×10^{-32} cm^6 s^{-1}			
	$^1P_1$ $(0.9 - 0.17) \times 10^{-32}$ cm^6 s^{-1}			
$X_2^{\star} \rightarrow 2X + h\nu$	$^1\Sigma_u^+$ $\zeta = 4.20 \pm 0.13$ ns	[66]	$\zeta = 6.22 \pm 0.80$ ns	[66]
	$^3\Sigma_u^+$ $\zeta = 2.88 \pm 0.06$ μs	[66]	$\zeta = 100 \pm 2$ ns	[66]
$^1\Sigma_u^+ + X \underset{-k}{\overset{k}{\rightleftarrows}} {}^3\Sigma_u^+ + X$	$k \leqslant 10^{-13}$ cm^3 s^{-1}	[52]		
	$< 10^{-14}$ cm^3 s^{-1}	[66]	$(1.25 \pm 0.68) \times 10^{-13}$ cm^3 s^{-1}	[66]
	$-k \leqslant 10^{-15}$ cm^3 s^{-1}	[8]		
	$< 1.8 \times 10^{-15}$ cm^3 s^{-1}	[66]	$(6.6 \pm 1.08) \times 10^{-15}$ cm^3 s^{-1}	[66]
$X^+ + 2X \rightarrow X_2^+ + X$	$(2.5 - 1.5) \times 10^{-31}$ cm^6 s^{-1}	[111] [112]	2.5×10^{-31} cm^6 s^{-1}	[66]
			$(2.0 - 3.6) \times 10^{-31}$ cm^6 s^{-1}	[109] [110]
$X_2^+ + e \rightarrow X^{\star\star} + X$	$3{,}4\ T_e^{-0.67} \times 10^{-5}$ cm^3 s^{-1}	[72]	$2.4\ T_e^{-0{,}5} \times 10^{-5}$ cm^3 s^{-1}	[72]
	$(7 \times 10^{-8}$ cm^3 s^{-1} at 10^4 K$)$		$(2 \times 10^{-7}$ cm^3 s^{-1} at 10^4 K$)$	
$X^{\star\star} + 2X \rightarrow X_2^{\star\star} + X$			10^{-31} cm^6 s^{-1}	[52]

TABLE VI — (Cont.)

Reaction	Ar	Ref.	Xe	Ref.
$X_2^{**} + (X) \rightarrow X^{*} + X + (X)$			10^{-11} cm^3 s^{-1}	[52]
$X_2^{*} + X_2^{*} \rightarrow 2X + X_2^{+} + e$	$\sim 10^{-9}$ cm^3 s^{-1}	[52]	$\sim 0.5 \times 10^{-9}$ cm^3 s^{-1}	[52]
$X_2^{*} + h\nu \rightarrow X_2^{+} + e$	$\sigma \sim 10^{-19}$ cm^2	[65]	$\sigma \sim 10^{-18}$ cm^2	[65]
$X(^3P_J) + e \rightleftarrows X(^3P'_J) + e$	(a) $10^{-6} - 10^{-7}$ cm^3 s^{-1}	[52]	$10^{-6} - 10^{-7}$ cm^3 s^{-1}	[52]
${}^3\Sigma_u^{+} + e \underset{-k'}{\overset{k'}{\rightleftarrows}} {}^1\Sigma_u^{+} + e$	(a) $10^{-6} - 10^{-7}$ cm^3 s^{-1}	[52]	$10^{-6} - 10^{-7}$ cm^3 s^{-1}	[52]
$X_2^{**}(^3\Sigma_u^{+}) + e \rightleftarrows X_2^{**} + e$	(a) $10^{-6} - 10^{-7}$ cm^3 s^{-1}	[52]	$10^{-6} - 10^{-7}$ cm^3 s^{-1}	[52]
$X^{**} + e \rightarrow X^{*} + e$	(a) $10^{-6} - 10^{-7}$ cm^3 s^{-1}	[52] [65]	$10^{-6} - 10^{-7}$ cm^3 s^{-1}	[52]
$X_2^{**} + e \rightarrow X_2^{*} + e$	(a) $10^{-6} - 10^{-7}$ cm^3 s^{-1}	[52] [65]	$10^{-6} - 10^{-7}$ cm^3 s^{-1}	[52] [65]
$X_2^{*} + e \rightarrow X_2^{+} + 2e$	(a) $10^{-7} - 10^{-8}$ cm^3 s^{-1}	[52] [65]	$10^{-7} - 10^{-8}$ cm^3 s^{-1}	[52]
$X_2^{*} + e \rightarrow 2X + e$	$\sim 10^{-9}$ cm^3 s^{-1}	[52] [65]	$\sim 10^{-9}$ cm^3 s^{-1}	[52]
$X^{**} \rightarrow X^{*} + h\nu$			1.5×10^{7} s^{-1}	[65]
$X^{**} + X \rightarrow X^{+} + X + e$			5×10^{-10} cm^3 s^{-1}	[65]
$X_2^{**} + X_2^{**} \rightarrow X_2^{+} + 2X + e$			5×10^{-10} cm^3 s^{-1}	[65]
$X^{*} + X^{+} \rightarrow X^{+} + X + e$			5×10^{-10} cm^3 s^{-1}	[65]

(a) Estimate dependent on T_e (ref. [52]).

A double star indicates a highly excited state.

Another kind of peculiar reactions, that may become very important are inelastic and superelastic collisions with excited species. Reactions such as

$$e + X\ ({}^{1,3}P_J) \rightleftarrows e + X\ ({}^{1,3}P_{J'})$$

$$e + X_2\ ({}^{3}\Sigma_u) \rightleftarrows e + X_2\ ({}^{1}\Sigma_u)$$

$${}^{1,3}\Sigma_u + e \rightleftarrows X_2^{\star\star} + e$$

originate a mixing of states and have rate constants of the order of $10^{-6} \cdot 10^{-7}$ cm^3 s^{-1}. Electronic states with energy differences of the order of 0.1 eV are completely mixed up and can be regarded as a unique state relaxing through the fastest way available for any one [52]. The excimer can be formed from ${}^{3,1}P_{2,1,0}$ but only the highest rate of formation is observed.

Experimental data for xenon and argon [52] [66] [99] [100] show that there is only a radiative lifetime that goes to a constant value as the pressure increases: a similar behaviour is expected for the other rare gases [52] and this is a result of the effect of the mixing reactions just mentioned.

The rate constants corresponding to the various reactions for this kinetic model for Xe and Ar are listed in table VI. This table was mainly taken from ref. [52] [65]. For some rate parameters, there are experimental values. For others, the values indicated are computed from the kinetic scheme displayed on fig. 14. Of course, cross sections of interaction of electrons with excited atoms or molecules are not known, and so there is still a lot of work to do in order to establish reliable rate constants for many reactions. Nevertheless, a reasonable understanding of the processes concerned is now believed to have been achieved.

5 — CONCLUDING REMARKS

As a conclusion, it must be emphasized as it comes out from the exposed, that the physical processes involved in the main mechanisms of production of both continua emission are thought to be known; however, their atomic precursors are not inequivocally established nor are the specific rate constants and/or cross sections of the reactions concerned, and for this reason a detailed and safe mechanism is still to be established. Very little spectroscopic information exists on the higher atomic excited states of the rare gases, the same being true for the higher excited states of the excimers. Mulliken has suggested [48] that radiative transitions could occur from higher excited molecular states (formed upon collision from the excited levels 2p or even 3p) to the levels $^3\Sigma_u^+$ and $^1\Sigma_u^+$. Experimental observations of these transitions do not practically exist [52] [99] except for the work of Firestone [46]. We must also remark that two other continua emission have been reported for argon by several authors, at 1900 Å and 2200 Å, weaker than those in the VUV [33], [57], [101]-[104].

While the first one is believed to belong to some impurity emitting in that region [99], the second one seems to have in fact a molecular origin, but conclusive studies are still lacking [101] [105]. It could be a recombination continuum [99] [105]. Huffman et al [106] observed a weak continuum emission at 850 Å which could correspond to direct emission from Ar_2^{**} to the repulsive ground state. To a clear understanding of the full process is essential more experimental work in a wider spectral region, including the 2p-1s and 3p-1s spectral lines.

We thank Prof. A. Policarpo for useful discussions.

Permission granted for the reproduction of the figures and tables taken from published work, as signaled 'in loco', is gratefully acknowledged.

Financial support given by Instituto Nacional de Investigação Científica (Centro de Física da Radiação e dos Materiais) is fully acknowledged.

REFERENCES

[1] J. B. BIRKS, The Theory and Practice of Scintillation Counting, Pergamon 1964.

[2] C. K. RHODES, *IEEE J. Quant. Elect.* **QE9**, 647 (1973).

[3] P. E. THIESS, G. H. MILEY, *IEEE Trans. Nucl. Sci.,* **NS21**, 125 (1974).

[4] R. D. ANDRESEN, E. A. LEIMANN, A. PEACOCK, *Nucl. Instr. and Meth.* **140**, 371 (1977).

[5] J. R. MCNEELY, G. S. HURST, E. B. WAGNER, M. G. PAYNE, *J. Chem. Phys.*, **63**, 2717 (1975).

[6] T. E. STEWART, G. S. HURST, D. M. BARTELL, J. E. PARKS, *Phys. Rev.*, **A3**, 1991 (1971).

[7] P. K. LEICHNER, *Phys. Rev.*, **A8**, 815 (1973).

[8] T. OKA, K.U.S. RAMA RAO, J. L. REDPATH, R. F. FIRESTONE, *J. Chem. Phys.*, **61**, 4740 (1974).

[9] L. G. CHRISTOPHOROU, Atomic and Molecular Radiation Physics, Wiley-Interscience, 1971.

[10] Y. TANAKA, K. YOSHINO, *J. Chem. Phys.*, **53**, 2012 (1970).

[11] G. A. ERSKINE, *Proc. Roy. Soc.*, **A224**, 362 (1954).

[12] L. R. PETERSON, J. E. ALLEN JR., *J. Chem. Phys.*, **56**, 6068 (1972).

[13] D. E. GERHART, *J. Chem. Phys.*, **62**, 821 (1975).

[14] M. INOKUTI, Y. K. KIM, R. L. PLATZMAN, *Phys. Rev.*, **164**, 55 (1967).

[15] M. INOKUTI, Y. ITIKAWA, J. E. TURNER, *Rev. Mod. Phys.*, **43**, 297 (1971); ibid, **50**, 23 (1978).

[16] E. EGGARTER, *J. Chem. Phys.*, **62**, 833 (1975).

[17] U. FANO, *Radiat. Res.*, **64**, 217 (1975).

[18] C. E. KLOTS, H. WRIGHT, *Int. J. Radiat. Phys. Chem.*, **2**, 191 (1970).

[19] J. A. R. SAMSON, F. L. KELLY, «Planetary Physics III: Photoionization Cross Sections of the Rare Gases» Geophysics Corporation of America Report GCA 64-3-N, Washington D. C., 1964.

[20] R. L. PLATZMAN, *Int. J. Appl. Radiat. Isot.*, **10**, 116 (1961).

[21] R. L. PLATZMAN, *J. Phys. Rad.*, **21**, 843 (1960).

[22] R. L. PLATZMAN, *Voltex*, **23**, 372 (1962).

[23] R. L. PLATZMAN, *Radiat. Res.*, **3**, 340 (1955); ibid, **2**, 1 (1955); ibid, **17**, 419 (1962); ibid, **32**, 383 (1967).

[24] R. L. PLATZMAN, Radiation Biology and Medicine, ch. 2, Addison-Wesley, Reading, Mass. (1958).

[25] K. M. SANDO, *Mol. Phys.*, **23**, 413 (1972).

[26] B. I. SCHNEIDER, J. S. COHEN, *Radiat. Res.*, **59**, 363 (1974).

[27] D. M. BARTELL, G. S. HURST, E. B. WAGNER, *Phys. Rev.*, **A7**, 1068 (1973).

[28] E. N. LASSETTRE, A. SKERBARLE, M. A. DILLON, K. J. ROSS, *J. Chem. Phys.*, **48**, 5066 (1968).

[29] H. BOERSCH, J. GEIGER, H. HELLWIG, *Phys. Letters.*, **3**, 64 (1962).

[30] N. F. Mott, H. S. W. Massey, The Theory of Atomic Collisions, Oxford 1965.

[31] R. Henck, Doctoral Thèse (Strasbourg 1966).

[32] V. Schmidt, N. Sandner, H. Kuntzemüller, *Phys. Rev.,* **A13**, 1743 (1976).

[33] W. R. Bennett Jr., *Ann. Phys.,* **18**, 367 (1962).

[34] R. Henck, R. Voltz, *J. Phys.,* **29**, 149 (1968).

[35] J. B. Hasteed, Physics of Atomic Collisions, Butherworths 1972.

[36] G. S. Hurst, C. E. Klots, *Advan. Rad. Chem.,* **5**, 1 (1976).

[37] J. Seguinot, T. Y. Ypsilantis, *Nucl. Inst. and Meth.,* **142**, 377 (1977).

[38] B. A. Dolgoshein, V. N. Lebedenko, A. M. Rogozhin, B. U. Rodionov, E. N. Shuvalova, *Soviet Physics* JETP **29**, 619 (1969).

[39] S. Konno, T. Takahashi, *Nucl. Inst. Meth.,* **150**, 517 (1978).

[40] S. Kubota, T. Takahashi, T. Doke, *Phys. Rev.,* **165**, 225 (1968).

[41] N. Thonnard, G. S. Hurst, *Phys. Rev.,* **A5**, 1110 (1972).

[42] T. E. Stewart, G. S. Hurst, T. E. Bortner, J. E. Parks, F. W. Martin, H. L. Weidner, *J. Opt. Soc. Am.,* **60**, 1290 (1970).

[43] A. Gedankan, J. Jortner, B. Raz, A. Szöke, *J. Chem. Phys.,* **57**, 3456 (1972).

[44] P. E. Thiess, Doctoral Thesis (Illinois 1975).

[45] Odile Dutuit, Thèse (docteur 3eme Cycle) (Orsay 1974).

[46] S. Arai, R. F. Firestone, *J. Chem. Phys.,* **50**, 4575 (1969).

[47] P. E. Thiess, G. H. Miley, *Tran. Am. Nucl. Soc.,* **18**, 70 (1974).

[48] R. S. Mulliken, *J. Chem. Phys.,* **52**, 5170 (1970).

[49] D. C. Lorents, R. E. Olson, G. M. Conklin, *Chem. Phys. Letters,* **20**, 589 (1973).

[50] T. L. Gilbert, A. L. Wahl, *J. Chem. Phys.,* **55**, 5247 (1971).

[51] I. M. Parson, P. E. Siska, Y. T. Lee, *J. Chem. Phys.,* **56**, 1511 (1972).

[52] D. C. Lorents, *Physica,* **82C**, 19 (1976).

[53] R. C. Michaelson, A. L. Smith, *J. Chem. Phys.,* **61**, 2567 (1974).

[54] Y. Tanaka, W. C. Walker, K. Yoshino, *J. Chem. Phys.,* **70**, 380 (1979).

[55] D. E. Freeman, K. Yoshino, Y. Tanaka, *J. Chem. Phys.* **71** 1780 (1979).

[56] B. Brocklehurst, *Radiat. Res. Reviews,* **1**, 223 (1968).

[57] M. Martin, *J. Chem. Phys.,* **54**, 3289 (1971).

[58] O. Cheshnovsky, B. Raz, J. Jortner, *Chem. Phys. Letters,* **15**, 475 (1972).

[59] H. U. Mittmann, H. P. Weise, *Z. Naturforsch.,* **29a**, 400 (1974).

[60] W. Aberth, D. C. Lorents, *Phys. Rev.,* **144**, 109 (1966).

[61] G. Klein, M. J. Carvalho, CRN/CPR 79-2.
Centre de Recherches Nucleaires et Université Louis Pasteur, Strasbourg.

[62] M. J. Carvalho, G. Klein, *J. Luminescence,* **18/19**, 487 (1979).

[63] G. Zimmerer, *J. Luminescence,* **18/19**, 875 (1979).

[64] R. S. Mulliken, *Radiat. Res.,* **59**, 357 (1974).

[65] D. C. Lorents, D. J. Eckstrom, D. Huestis, Excimer Formation and Decay Processes in Rare Gases.
Final Report MP 73-2, Contract N00014-72-C-0457, SRI Project 2018, Stanford Research Institute, Menlo Park Ca (1973).

[66] J. W. Keto, R. E. Gleason Jr., T. D. Bonifield, G. K. Walters, F. K. Soley, *Chem. Phys. Letters,* **42**, 125 (1976).

[67] E. Collier, International Conference on VUV, Montpellier 1977.

[68] U. Hahn, N. Schwentner, G. Zimmerer, *Opt. Communic.,* **21**, 237 (1977).

[69] H. S. W. Massey, E. H. S. Burhop, H. B. Gilbody, Electronic and Ionic Impact Phenomena. Oxford University Press.

[70] E. C. Beaty, P. Patterson, 6th Intern. Conf. on Ionization Phenomena in Gases, **1**, SERMA Paris, 289 (1963).

[71] F. Liu Wei-Cheng, D. C. Conway, *J. Chem. Phys.,* **60**, 784 (1974).

[72] J. N. Bardsley, M. A. Biondi, Advances in Atomic and Molecular Physics, **6** (1970). Editors D. R. Bates, I. Estermann. Academic Press, New York.

[73] J. Y. Shiu, M. A. Biondi, *Phys. Rev.,* **A17**, 868 (1978); ibid **A16**, 1817 (1977).

[74] Y. J. Shiu, M. A. Biondi, D. P. Sipler, *Phys. Rev.,* **15**, 494 (1977).

[75] T. Holstein, *Phys. Rev.,* **72**, 1212 (1947); ibid, **83**, 1159 (1951).

[76] G. M. Lawrence, *Phys. Rev.,* **175**, 40 (1968).

[77] P. G. Wilkinson, *Can. J. Phys.,* **45**, 1715 (1967).

[78] R. A. Nodwell, J. Meyer, T. Jacobson, *J. Quant. Spectrosc. Radiat. Transfer,* **10**, 335 (1970).

[79] J. R. Bennett, A. J. L. Collinson, *J. Phys.,* **B2**, 571 (1969).

[80] J. A. Hornbeck, J. P. Molnar, *Phys. Rev.,* **84**, 621 (1951).

[81] G. S. HURST, T. E. STEWART, J. E. PARKS, *Phys. Rev.*, **A2**, 1717 (1970).

[82] R. E. HUFFMAN, D. H. KATAYAMA, *J. Chem. Phys.*, **45**, 138 (1966).

[83] H. HELM, K. STEPHAN, T. D. MÄRK, *Phys. Rev.*, **A19**, 2154 (1979).

[84] O. CHESHNOVSKY, B. RAZ, J. JORTNER, *J. Chem. Phys.*, **59**, 3301 (1973).

[85] Y. TANAKA, K. YOSHINO, D. E. FREEMAN, *J. Chem. Phys.*, **62**, 4484 (1975).

[86] D. E. FREEMAN, K. YOSHINO, Y. TANAKA, *J. Chem. Phys.*, **67**, 3462 (1977).

[87] N. LEE, J. B. FENN, *Rev. Sci. Instr.*, **49**, 1269 (1978).

[88] P. M. DEHMER, J. L. DEHMER, *J. Chem. Phys.*, **68**, 3462 (1978).

[89] G. S. HURST, E. B. WAGNER, M. G. PAYNE, *J. Chem. Phys.*, **61**, 3680 (1974).

[90] R. C. MICHAELSON, A. L. SMITH, *Chem. Phys. Letters*, **6**, 1 (1970).

[91] E. ELLIS, N. D. TWIDDY, *J. Phys.*, **B2**, 1366 (1969).

[92] R. BOUCIQUE, P. MORTIER, *J. Phys.*, **D3**, 1905 (1970).

[93] W. WIENNE, J. WIENNE-LENAERTS, *Phys. Letters*, **47A**, 37 (1974).

[94] R. F. FIRESTONE, Report No **C00-1116-20**, Ohio State University (1972).

[95] J. LE CALVÉ, R. A. GUTCHECK, O. DUTUIT, *Chem. Phys. Letters*, **47**, 470 (1977).

[96] M. G. PAYNE, (unpublished results — see ref. [36]).

[97] P. MOERMAN, R. BOUCIQUÉ, P. MORTIER, *Phys. Letters*, **49A**, 179 (1974).

[98] J. W. KETO, R. E. GLEASON Jr., G. K. WALTERS, *Phys. Rev. Letters*, **33**, 1365 (1974).

[99] H. A. KOEHLER, L. J. FERBERDER, D. L. READHEAD, P. J. EBERT, *Phys. Rev.*, **A9**, 768 (1974).

[100] J. B. GERARDO, A. W. JOHNSON, *J. Quant. Elect.* **QE9**, 748 (1973).

[101] G. S. HURST, T. E. BORTNER, T. D. STRICKLER, *Phys. Rev.*, **49**, 2460 (1968); ibid, **178**, 4 (1969).

[102] J. JORTNER, L. MEYER, S. A. RICE, E. G. WILSON, *J. Chem. Phys.*, **42**, 4250 (1965).

[103] T. D. STRICKLER, E. T. ARAKAWA, *J. Chem. Phys.*, **41**, 1783 (1964).

[104] J. R. BENNETT, A. J. L. COLLINSON, *J. Phys.*, **B2**, 571 (1969).

[105] J. A. VIECELLI, UCRL Report No **UCRL-51374** (1973), (unpublished).

[106] R. E. Huffman, Y. Tanaka, J. C. Larrabee, *J. Opt. Soc. Am.*, **52**, 851 (1962).

[107] B. Schneider, J. S. Cohen, *J. Chem. Phys.*, **61**, 3240 (1974).

[108] P. K. Leichner, R. J. Ericson, *Phys. Rev.*, **A9**, 251 (1974).

[109] D. Smith, A. G. Dean, I. C. Plumb, *J. Phys.*, **B5**, 2134 (1972).

[110] A. P. Vitols, H. J. Oskam, *Phys. Rev.*, **A8**, 1860 (1973).

[111] D. Smith, P. R. Cromey, *J. Phys.*, **B1**, 638 (1968).

[112] C. B. Kretschmer, H. L. Pederson, *J. Appl. Phys.*, **34**, 3209 (1963).

[113] A. V. Phelps, J. P. Molnar, *Phys. Rev.*, **89**, 1202 (1953).

[114] A. H. Futch, F. A. Grant, *Phys. Rev.*, **104**, 356 (1956).

[115] J. Le Calvé, M. Bourène, *J. Chem. Phys.*, **58**, 1446 (1973).

[116] M. Bourène, J. Le Calvé, *J. Chem. Phys.*, **58**, 1452 (1973).

[117] L. Colli, *Phys. Rev.*, **95**, 892 (1954).

[118] M. Bourène, O. Dutuit, J. Le Calvé, *J. Chem. Phys.*, **63**, 1668 (1975).

[119] N. Sadegui, IV Coll. Nat. Phys. Collisions Atomiques et Electroniques, Brest (1970).

[120] R. A. Gutchek, E. C. Zipf, *Bull. Am. Phys., Soc.*, **17**, 395 (1972).

[121] M. G. Payne, J. E. Talmage, G. S. Hurst, E. B. Wagner, *Phys. Rev.* **A9**, 1050 (1974).